JBC Papers in Press. Published on November 5, 2009 as Manuscript M109.017491
The latest version is at http://www.jbc.org/cgi/doi/10.1074/jbc.M109.017491

Decreased superoxide production in macrophages of long-lived p66Shc-knockout mice

Alexey A. Tomilov, Vincent Bicocca, Robert A. Schoenfeld, Marco Giorgio*, Enrica Migliaccio*, Jon J. Ramsey, Kevork Hagopian, Pier Giuseppe Pelicci* and Gino A. Cortopassi

VM: Molecular Biosciences, UC Davis, CA 95616
*European Institute for Oncology, Milan, Italy

Address correspondence to: Gino Cortopassi, PhD., 1120 Haring hall, Davis, CA 95616, Fax (530) 754-9342, Email: gcortopassi@ucdavis.edu

Keywords: NADPH Oxidase, superoxide, longevity, macrophage, inhibitors, p66Shc, knockout, signaling

Abstract.

A decrease in Reactive Oxygen Species (ROS) production has been associated with extended lifespan in animal models of longevity. Mice deficient in the p66Shc gene are long-lived, and their cells are both resistant to oxidative stress and produce less ROS. Our microarray analysis of p66Shc(-/-) mouse tissues showed alterations in transcripts involved in heme and superoxide production and insulin signaling. Thus we carried out analysis of ROS production by NADPH Oxidase (PHOX) in macrophages of control and p66Shc-knockout mice. p66Shc(-/-) mice had a 40% reduction in PHOX-dependent superoxide production. To confirm whether the defect in superoxide production was a direct consequence of p66Shc deficiency, p66Shc was knocked down with siRNA in the macrophage cell line RAW264, and a 30% defect in superoxide generation was observed. The pathway of PHOX-dependent superoxide generation was investigated. PHOX protein levels were not decreased in mutant macrophages, however the rate and extent of phosphorylation of p47phox was decreased in mutants, as was membrane translocation of the complex. Consistently phosphorylation of protein kinase C delta, Akt and ERK (the kinases responsible for phosphorylation of p47phox) was decreased. Thus, p66Shc deficiency causes a defect in activation of the PHOX complex that results in decreased superoxide production. p66Shc-deficient mice have recently been observed to be resistant to atherosclerosis, and oxidant injury in kidney and brain. Since phagocyte-derived superoxide is often a component of oxidant injury and inflammation, we suggest that the decreased superoxide production by PHOX in p66Shc-deficient mice could contribute significantly to their relative protection from oxidant injury, and consequent longevity.

Introduction

The free radical theory of aging predicts that Oxygen-derived free radicals produced throughout life causes progressive damage and inflammation ultimately leading to death [1]. In the long-lived p66Shc-deficient mouse, embryonic fibroblasts produce less ROS and are more resistant to stressors including hydrogen peroxide, and signal less through ROS-dependent pathways [2, 3]. p66Shc-deficient mice produce less mitochondrial ROS following CCl_4 stimulation [4]. p66ShcKO mice also have reduced systemic and tissue oxidative stress [5], and are resistant to atherosclerosis [6], oxidant-related endothelial dysfunction [7], kidney oxidant injury [8], and are protected from high fat diet induced obesity [3].

We carried out a microarray study that indicated alterations in transcripts related to heme and NADPH Oxidase superoxide production, and so investigated the impact of the p66Shc-deficiency on ROS generating activity of macrophages.

Experimental procedures

Animals p66Shc(-/-) mice have being described previously [2]. Mice were kept pathogen-free through the study on barrier facility at UC Davis. All experimental procedures were approved by the Institutional Animal Care and Use Committee (IACUC) and were performed in compliance with local, state, and federal regulations. Mice, used for this study were 2-6 month old and were age matched for each experiment.

Antibodies and reagents Diphenyleneiodonium (DPI) and Gliotoxin was purchased from Axxora LLC (San Diego, CA), Phorbol 12-myristate 13-acetate (PMA) was from Enzo Life Sciences International INC. (Plymouth Meeting, PA), N-formil-Met-Leu-Phe (fMLP) was from Tocris Bioscience (Ellisville, MO), arachidonic acid (AA) was from Acros Organics (Morris Plains, NJ), OxyBURST Green H2HFF-BSA dye was purchased from Molecular Probes (Eugene, Oregon), goat anti-p22Phox antibody was from Santa Cruz Biotechnology INC. (Santa Cruz, CA), rabbit anti-p40Phox polyclonal and rabbit anti-p67Phox polyclonal antibodies were from Upstate Cell Signaling Solutions (Lake Placid, NY), rabbit anti-phospho p40Phox polyclonal antibody were from Cell Signaling Technology INC. (Danvers, MA), goat anti-p47Phox polyclonal, goat anti-Rac2 polyclonal, rabbit anti-PKC delta polyclonal and rabbit anti-phospho-PKC delta monoclonal antibody was from Abcam INC. (Cambrige, MA), rabbit anti-Shc polyclonal antibodies and mouse anti-gp91Phox antibody was from BD Biosciences (San Diego, CA), Rac/cdc42 Assay reagent PAK-1 PBD agarose conjugate and mouse monoclonal anti-Rac1 antibody were from Millipore INC. (Temecula, CA), goat anti – rabbit monoclonal antibody labeled with IR-dye 700CW, donkey anti-mouse monoclonal antibody labeled with IR-dye 800CW and donkey anti-goat polyclonal antibodies, conjugated with IR-dye 800CW were from Li-Cor Biosciences (Lincoln, NE). Primers for quantification of p66Shc forward 5'-

gaaagttggggcggtgac-3' and reverse 5'-gacccattctgcctcctc-3', actin beta forward 5'-tggaacggtgaaggcgacagcagttg-3' and reverse 5'-gtggcttttgggagggtgagggactt-3', p66Shc specific siRNA [9] were synthesized on Integrated DNA Technology (Coralville, IA), non-target control siRNA-AllStar was purchased from Qiagen (Valencia, CA). RAW264.7-cells were from ATCC (Manassas, VA), Bio-Lyte 5/8 and Bio-Lyte 3/10 Ampholytes were from Bio-Rad laboratories (Hercules, CA).

Peritoneal macrophages-- (PM) were harvested 4 days after thioglycollate injection of the peritoneal cavity. Cells were washed with chilled PBS, red blood cells were hypotonically lysed and macrophages were resuspended in RPMI 1640 containing 15% FBS, 50 μg/ml penicillin and 50 μg/ml streptomycin and plated on 100 mm round Petri - dishes. After 2 hours incubation at 37°C, 5% CO_2 non-adherent cells were removed and the remaining adherent cells were cultured in RPMI 1640 containing 15% FBS, 50 μg/ml penicillin, and 50 μg/ml streptomycin for no more than 48 hours before functional assays.

Tissue culture—RAW264.7 cells were cultured in RPMI 1640 containing 15% FBS, 50 μg/ml penicillin and 50 μg/ml streptomycin, and sub-cultured twice a week.

RNA isolation and Semi-quantitative RTPCR – Total RNA was extracted by direct lysis of the cells on the tissue culture plate using RNeasy Mini Kit (Qiagen) according to manufacturer's instructions. Equal RNA amounts were added to Superscript II First Strand reverse transcriptase reaction mixture (Invitrogen) with oligo(dT) primer. The resulting templates were subject to Syber Green-based quantitative PCR using specific primers, listed above. The cycling conditions were 94°C 3 minutes as initial denaturation followed by 35 cycles of 94°C 15 second, 60°C 20 second and 72°C 15 second and finished by melting curve by gradual heating until 95°C. Only experiments with a single melting peak were considered for analysis. Reaction qualities have being verified by gel electrophoresis. PCR was carried out using LightCycler480 Real time PCR instrument and LightCycler480 analysis software (Roshe).

Blood heme measurement was performed on heart blood samples. Blood was collected in capillary tubes containing electrolyte-balanced heparin at 70 IU/ml of blood. Following collection, blood samples were immediately analyzed for hemoglobin levels on Radiometer OSM3 Hemoximeter (Copenhagen, Denmark).

Superoxide production by RAW264.7 cells – Cells were cultivated and transfected on 6 well plates (Nunc) started at two hundred thousand cells per well. Transfection was performed as described, and after 48 hours cells were washed with PBS pH 7.4 at 37°C, and 3 ml of KRP, which contains PBS pH 7.4, 1 mM $CaCl_2$, 1.5 mM $MgCl_2$, 5.5 mM glucose and 10 μg/ml OxyBURST H_2HFF Green BSA dye was added. Cells were incubated at 37°C in the dark for two minutes and readings of fluorescence at 530 nm exited at 480 nm were taken during 12 minutes using CytoFluor Multi-Well Plate Reader (PerSeptive Biosystems), then PMA until 3 μg/ml was added to experimental wells and readings were continued during next 30 minutes, DMSO (solvent for PMA) was added to control cells, used as baseline. After the assay, one half of the cells from each well were taken to the cell count and trypan blue based viability assay, and the number of cells in each well was calculated. Fluorescence readings were normalized to exact viable cell number in each well. Another half of the cells were used for either: protein extraction for Western Blots, or total RNA extraction for Semi-quantitative Reverse Transcriptase-PCR.
For the Gliotoxin or DPI inhibition of NAD(P)H-oxidase, Gliotoxin or DPI were directly added to the tissue culture media until final concentration of 10 μg/ml for Gliotoxin or 10 μM for DPI, and cells were pre-incubated during 10 minutes at 37°C prior to measurements of superoxide production.

Superoxide production by Mouse Peritoneal Macrophages (PM) – For the H_2HFF-based assay cells were cultivated at 37°C and 5% CO_2 on 100 mm tissue culture dishes for 24-48 hours after harvesting. Media was RPMI 1640 containing 15% FBS, 50 μg/ml penicillin, 50 μg/ml streptomycin. Cells were washed with ice-cold PBS pH7.4 and resuspended in ice-cold KRP. Aliquots were taken for cell counting and viability assay, exact number of cells was calculated. Indicated number of cells was taken into warm 96 well plate with fresh KRP supplemented with OxyBURST H_2HFF Green BSA dye until 10 μg/ml, final volume was 190 μl. After two minutes incubation in the dark readings were started at emission 530 nm and excitation of 480 nm. Stimulus: PMA until 3 μg/ml, fMLP until 3 μM or AA until 15 μM were added at minute 12, and readings were continued during next 30 minutes. Ten seconds mixing step was used in each reading cycle of the

instrument to prevent the cells from sedimentation. Gliotoxin or DPI inhibition was done similarly as described above.

For SOD-inhibitable cytochrome c reduction based assay PM were harvested from peritoneal cavity 4 days after thioglycollate injection by lavage with ice-cold PBS. Contaminating erythrocytes were hypotonically lysed and PM were resuspended in KRP, pH 7.4 at $5X10^6$ cells per ml and kept on ice until use. The reaction mixture was 250 µl and contained 50 µM cytochrome c and $6.25X10^5$ PM in KRP. The superoxide release was induced with 4 µg of PMA and readings of absorbance at 550 nm were taken during 10 minutes using Tecan Spectra Rainbow 96 well plate spectrophotometer (Tecan, Austria). The same assay was carried out in the presence of SOD at 2.5 µg per reaction in order to evaluate the superoxide independent change in absorbance. A sample without PMA was used as a negative control.

siRNA transfection of RAW264.7 cells was carried out on 6 well plates (Nunc). Two hundred thousand cells per well were plated in antibiotic free RPMI 1640 15% FBS and after settlement washed with PBS. Transfection mixture was prepared using 70 nM siRNA specific for p66Shc or non-specific AllStar siRNA (Qiagen), OPTIMEM media (Invitrogen) and Lipofectamine 2000 (Invitrogen) according to manufacturer protocol. After six hours of transfection in 600 µl of transfection mixture per well, cells were feed with fresh RPMI 1640 supplemented with 15% FBS. After 48 hours of cultivation cells were used in NAD(P)H-oxidase measurement assays followed by cell counting and RNA or protein extraction as described above.

Microarray analysis of differently regulated transcripts – Total RNA was extracted from following tissues of individual age matched mouse: liver, spleen, lungs, epididymal fat, PM, at 3 month of age and liver, retroperitoneal fat, and spleen at 12 month of age, using TRIzol reagent according to the manufacturer instructions (Invitrogen), then purified using RNeasy Mini Kit (Qiagen). Two mutant and two control mice were used for each experiment. Totally 16 samples from mutant mice and 16 samples from control mice tissues were used. First and second strand of cDNA were generated using One-Cycle cDNA Synthesis Kit (Affymetrix), labeled cRNA's were synthesized using Gene Chip IVT Labeling System (Affymetrix), fragmented and hybridized to the Mouse Genome 430 2.0 Arrays (Affymetrix) according to manufacturer instructions. Resulted CEL files were analyzed for each group of tissue individually using dChip (DNA chip analyzer) software [10]. Updated annotations were obtained from the NetAffx database and multi-sample analysis performed by combining the dChip lists using Excel. Probsets with a pCall >20% and $p < 0.05$ were considered significantly altered.

An additional set of CEL files was obtained from the Pelicci group. Liver, spleen and lungs samples from 3 month old p66Shc(-/-) and 3 month old control mice were hybridized in a similar way to the Affymetrix Mouse Genome U74Av2 chips. RNA samples of each tissue from three animals were pulled together. Two chips for each RNA sample of control and two chips for each RNA sample of mutant mice were used. The CEL files were analyzed with dChip in our laboratory and incorporated into our expression data table using >90% probsets match between two different chips formats Mouse Genome 430 2.0 and U74Av2. Probesets were then resorted by number of times to be significantly changed through different experiments. Lists of top 250 up- and 250 down-regulated genes were categorized using Onto-Express Pathway analysis tool and lists of 100 top up- and 100 top down-regulated genes were categorized using Onto-Express Bioprocess analysis tool [11]. For filtering OntoExpress results we used cutoff for p-value 0.05. Lists of significantly altered pathways counting 27 and significantly altered bioprocesses – 18 were sorted by impact factor and p-value respectively, and fore top up- and fore top down-regulated were tabulated.

Western Blotting – Total protein was isolated by direct lysis of adherent cells or from cell pellets washed with ice-cold PBS pH7.4 using Cell Lysis buffer (Cell Signaling Technologies), containing 20 mM Tris-HCl (pH 7.5) 150 mM NaCl, 1 mM Na_2EDTA, 1 mM EGTA, 1% Triton, 2.5 mM sodium pyrophosphate, 1mM β-glycerophosphate, 1 mM Na_3VO_4, 1 µg/ml leupeptin, 1mM Phenylmethanesulfonyl fluoride and supplemented with Complete Mini Protease Inhibitor Cocktail and PhosStop Phosphatase Inhibitor Cocktail (Roshe). Forty microgram of protein per line, as determined by Bradford assay (BioRad Laboratories), were resolved by SDS-PAGE, transferred to nitrocellulose membrane, blocked with Odyssey Blocking Buffer (Li-Cor Biosciences) and hybridized with indicated primary antibodies followed by development with infrared IR-dye 700CW and/or 800CW labeled secondary antibodies (Li-Cor). Blots were scanned on Licor Odyssey infrared imaging instrument and quantified using Odyssey 2.1 software. Use of

different IR-dyes labeled secondary antibodies allowed to measure level of housekeeping proteins at the same time as the proteins of interest on the same membrane and improves accuracy of quantification and normalization.

Two dimensional electrophoresis – Macrophages were induced with DMSO (Mock treatment) or PMA for 5 minutes, as indicated, reactions were stopped with 5 volumes of ice-cold PBS; cells were collected by quick centrifugation at 0°C and lysed by sonication with First Dimension Buffer containing 8.0M Urea, 2.0% Triton X-100, 5% β-mercaptoethanol, 1.6% Bio-Lyte 5/7 and 0.4% Bio-Lyte3/10 ampholytes, 1,5% CHAPS. Samples were isoelectrofocused on 4% PAGE (T=25%, C=3%), supplemented with 8M Urea 1.5% CHAPS at pH range of 4 – 9. Isoelectrofocusing gels were than transferred on top of gradient 4 – 15% SDS – PAGE for second dimension. Blots were probed with Goat anti – p47phox antibody. For the second hybridization, blots were probed with Donkey anti – Goat monoclonal antibodies (Li-Cor), labeled with IR – dye 800CW. Membrane was scanned with infrared scanner Licor Odyssey and analyzed with Odyssey 2.1 software.

Sub fractionation of protein extracts – Total protein was isolated from control and p66Shc(-/-) PM induced with PMA for 5 minutes or mock treated as described above. Cells were collected and lysed by 20 strokes in CHAPS lysis buffer containing 20mM Tris-HCl (pH 7.5), 150 mM NaCl, 10% Glycerol, 0.5% CHAPS and supplemented with Complete Mini Protease Inhibitor Cocktail and PhosStop Phosphatase Inhibitor Cocktail (Roshe). Unbroken cells were collected by brief centrifugation at 400g and protein concentrations were determined. 100 µg of total protein were adjusted to 60 µl with CHAPS lysis buffer and centrifuged at one hundred thousand gravity force during 30 minutes at +4°C. Supernatant was called cytosolic fraction and pellet was washed with CHAPS lysis buffer and contained membrane fraction of proteins. Cytosolic fraction was supplemented until 1X with Laemmli Sample Buffer, membrane fraction was resuspended in 1X Laemmli Sample Buffer. Fractions were boiled till dissolved completely and loaded on SDS PAGE. Western Blots with indicated antibody were performed as described above.

Rac activation assay – Macrophages were isolated from 3 month old mice as described above and $7X10^6$ cells were resuspended in 6 ml of KRP media. Three ml of cell suspension were induced with stimulus: 3 µg/ml of PMA for 5 minutes or 5 µM fMLP for 60 seconds, as indicated; other half of three ml cell suspension were treated with equal amount of DMSO (Mock treatment). For fMLP induction cells were pretreated with 10 µM cytochalasin b for 10 minutes. Reactions were stopped by 5 volumes dilution of ice cold PBS, cells were collected by rapid centrifugation and lysed in ice cold lysis buffer: 25 mM HEPES pH=7.5, 150mM NaCl, 1% Igepal CA 630, 10% glycerol, 25 mM NaF, 10 mM $MgCl_2$, 1 mM EDTA, 1 mM Sodium orthovanadate, and Complete Mini proteinase inhibitor cocktail (Roshe, Mannheim). Lysates were rapidly clarified by low speed centrifugation at +4°C and immediately frozen in liquid nitrogen until use. Aliquots of protein lysates were left for protein quantification.

GTP-Rac1/2 was precipitated using Rac/cdc41 Assay Reagent PAK-1 PBD agarose conjugate (Millipore, Temecula, CA) from equal amounts of protein as recommended by manufacturer. For the positive controls 1/3 aliquots of each experimental sample were loaded with 100 µM of GTPγS for 10 minutes at 30°C and than used for precipitation with PAK-1 PBD agarose. Positive control samples were used to estimate total Rac available for GTP-binding in a sample and to ensure that affinity reagent is not saturated. Precipitates were resolved on 15% SDS PAGE, and blots were probed with mouse anti-Rac1 monoclonal (Millipore, Temecula, CA) and Goat anti-Rac2 polyclonal antibody (Abcam Inc, Cambridge, MA). Blots were developed and quantified using infrared labeled secondary antibodies as described above. Fluorescent arbitrary units from Rac bands were normalized to a 50 kD constitutive band of constant intensity between all samples regardless GTPγS loading of lysates.

Results

p66Shc-deficient mice have transcriptional alterations in phosphatidylinositol and heme pathways.

To identify transcripts altered in long-lived p66Shc knockout mice, we microarrayed RNA from liver, spleen, lungs, fat and peritoneal macrophages, of 3 month old males and 12 month old males and females

of p66Shc(-/-) and control mice. A total of 19 mutants- and 19 age/sex-matched control animals were used for the hybridization with Affymetrix oligo-microarray chips followed by analysis of gene expression data using dChip [10]. Each dataset was analyzed individually and transcripts of $p< 0.05$, were organized in a megatable, and the top 250 up- and down-regulated genes were entered into OntoExpress [12] as described in methods. The top four significantly altered pathways are presented. Also, lists of top 100 up- and down- regulated genes were analyzed with OntoExpress for biological process [11]. Table of the top four regulated bioprocesses are shown (Table 1).

PI3Kinase and antigen processing were significantly altered pathways, impact factors 35 and 28, and heme transcripts were preferentially affected. Some of the genes underlying these down-regulated processes were related to NADPH Oxidase activity. Given the involvement of heme in NADPH Oxidase-dependent ROS production, this activity was specifically measured.

p66Shc(-/-) macrophages have a defect in NAD(P)H oxidase dependent ROS generation.

NADPH oxidase (PHOX) is the basis of the respiratory burst. We measured the respiratory burst of p66Shc(-/-) peritoneal macrophages by two different methods: the conventional SOD-inhibitable reduction of cytochrome *c* assay, and a more sensitive, fluorescence-based H_2HFF-oxidation assay, (Figure 1). Both H_2HFF dye oxidation and cytochrome c reduction were inhibitable with diphenyliodonium (DPI) or gliotoxin, specific PHOX inhibitors [13-16]. As determined by the cytochrome *c* assay, mean values of SOD-inhibitable superoxide production by 600,000 PMA-induced control macrophages was 151 pMol superoxide/minute, whereas p66Shc(-/-) macrophages produce 104 pMol superoxide/min. Thus, mutant macrophages have 69% of the NAD(P)H – oxidase activity of control. The difference in means was significant, $p<0.000003$ (Figure 2A). Similarly, the H_2HFF oxidation method demonstrated about 40% defect in superoxide production by mutant macrophages, p value 0.01084 (Figure 2 B). Similar results were obtained for fMLP and arachidonic acid (AA)-stimulated macrophages (Figure 2 C, D). Similar results were also obtained for p66Shc(-/-) mice in the 129 genetic background using the DCFDA assay.

P66Shc-null mice have no defects in expression levels of NOX2 subunits.

There are at least three explanations for a p66Shc-dependent defect in PMA-stimulated NAD(P)H – oxidase activity, i.e. a defect in expression in a PHOX component, in the heme necessary for superoxide production, or the rate of activation of the complex. First, we investigated the expression of the components of NOX2 complex, i.e. Rac1/2, p40phox, p47phox, p67phox p22phox or gp91phox, using western blots of protein extracts from peritoneal macrophages of p66Shc(-/-) and control mice (Figure 3 and data not shown). There was no significant decrease in protein levels of any tested NOX2 subunit in mutant macrophages versus control. Thus, the defect in PHOX activity in mutant p66Shc(-/-) cells could not be explained by a defect in NOX2 subunit levels.

Heme levels are unchanged in mutant mice blood. Heme deficiency causes delayed maturation and degradation of gp91phox, result in reduced gp91phox protein level in mammalian cells [17, 18]. Microarray results suggested a heme defect in p66Shc mice. However, since there was no difference between gp91phox abundance in mutant and control macrophages, it was unlikely that heme level would be different in p66Shc(-/-) mice. We investigated total blood heme levels, in p66Shc(-/-) mice vs. littermate controls. No significant difference was observed (Figure 4).

p66Shc(-/-) cells have reduced phosphorylation of p47phox. Since there was no deficiency in expression of cytosolic NOX2 subunits in the p66Shc(-/-) mice, no deficiency in membrane subunit gp91phox, and no heme deficiency, remaining explanations for the decreased level of PHOX activity included a reduction in phosphorylation of the main regulatory subunit p47phox, or reduced Rac – activation. After induction of macrophages with PMA or fMLP, p47phox becomes rapidly phosphorylated. The autoinhibitory domain [19] of p47phox contains four clusters of serine residues. Each cluster contains two or three Ser residues, separated by few amino – acids (ten serines totally) [20]. This phosphorylation induces the ultimate translocation of p47phox and p67phox, existing as a complex with p40phox in cytosol, to the heme-containing catalytic subunit gp91phox. The phosphorylation rate of p47phox is one of the limiting steps for the assembly and activation of PHOX [21]. The last phosphorylation step occurs only after p47phox translocates and associates with p22phox [22]. At the same time, GDP-GTP exchange factors Rac1 or Rac2 activate and translocates to the cytochrome b_{558}.

We measured phosphorylation rates of p47phox in PMA-induced macrophages from p66Shc(-/-) and control macrophages by two dimensional electrophoresis, as described in methods, followed by western blot with anti-p47phox antibody (Figure 5 A). The isoelectric point (IEF) for non – phosphorylated p47phox is 9.07. Upon phosphorylation, the IEF of the protein shifts towards acidic pH due to increasing number of PO_4^{3-} residues attached to the protein.

On mock treatment without PMA we observed a spot at molecular mass 47 kD and pH about 9, corresponding to p47phox and labeled with state "0" of phosphorylation. Upon PMA treatment for 5 minutes 4 spots appeared at molecular mass 47 kD with more acidic IEF, corresponding to higher phosphorylation states of p47phox. While only 22% of p47phox from wild-type PM remained unphosphorylated after 5 minutes treatment with PMA, 55% from mutant PM was unphosphorylated ((Figure 5 B). Consistently, mutants had about a 40% decrease in the phosphorylated isoforms of p47phox. Of the phosphorylated forms, p66Shc mutants had a higher fraction of p47phox in state 1 and 2 (30%) than controls that had a higher fraction of p47phox in phosphorylation states 3 and 4. Since the final phosphorylation step of p47phox occurs only after PHOX is fully assembled, we suggest that assembly of NAD(P)H – oxidase is reduced in p66Shc(-/-) cells. The 40% reduction in phosphorylation rate is sufficient to explain the 40% reduced rate of ROS production from p66Shc-deficient mice.

p66Shc(-/-) macrophages have reduced translocation of p47phox. We investigated PMA inducible translocation of p47phox to plasma membrane using ultracentrifugation to separate total protein from mutant and control macrophages on membrane and cytosolic fractions in five experiments. Cytosolic and membrane fractions were then resolved on SDS PAGE, a very slight MnSOD signal was observed in membrane fraction of PM protein extracts from both mutant and control mice, supporting that only very slight contamination (<1%) of membrane fraction by proteins from cytosolic fraction occurred. Beta actin bands (loading control) were present in all fractions. P47phox was about 35% less abundant membrane fractions of PMA-stimulated mutant macrophages vs. controls. Mock treated PM had similar levels of p47phox in membrane fraction. In some experiments membrane fractions were sonicated with SDS prior to SDS PAGE analysis, under these conditions membrane p47phox fraction migrated at the same molecular weight as cytosolic p47phox, demonstrating the PMA-dependent shift in p47phox's molecular weight (Figure 6) and data not shown).

The proteins for the experiment were isolated under mild lysis conditions with agent CHAPS in concentration of 0.5% as described in materials and methods (Fig. 6). After centrifugation of cleared lysates at 100,000*g* precipitates of membrane-associated proteins were tight and hard to dissolve. On the blot presented the shift in membrane fraction p47phox mobility on SDS-PAGE is large; also, p47phox runs as a doublet. We suggest that this was the result of incomplete penetration of loading buffer components into the pellet. We performed five similar independent experiments in which precipitates of membrane fraction were sonicated in loading buffer, boiled and loaded on the gel. The shift in mobility of p47phox was also apparent under these conditions, and membrane-associated p47phox was running at its expected mass as single band. We present the blot where membrane-associated p47phox ran slower because we suggest that this shift in mobility provides one more internal control for contamination of membrane fraction by cytosolic fraction. The doublet bands corresponding to membrane-associated p47phox were added and normalized to beta actin levels to correct for loading.

We suggest that reduced translocation of p47phox in mutant cells is the result of reduced phosphorylation of p47phox in p66Shc(-/-) mice, and could explain reduced superoxide generation by PM from p66Shc(-/-) mice.

siRNA-mediated p66Shc knockdown decreases NADPH-oxidase dependent superoxide generation. To address whether the defect in NADPH Oxidase-dependent superoxide production was a direct consequence of p66Shc, we knocked down p66Shc in the mouse macrophage cell line RAW264. In 25 independent transfections, we observed a mean reduction p66Shc of 40% and 60% at the mRNA and protein levels, respectively (Figure 7). P66Shc siRNA did not affect expression of NADPH-oxidase subunits or other p52 kD and p46 kD Shc isoforms at the protein level (Figure 7 and data not shown). The p66Shc – silenced RAW264.7 cells has about 30% reduction in PMA – inducible H_2HFF dye oxidation, which was inhibitable with DPI or Gliotoxin. We conclude that p66Shc deficiency is sufficient for partial defect in activation of NAD(P)H – oxidase.

p66Shc(-/-) macrophages do not have a big defect in Rac activation. Another component of NADPH oxidase activation in phagocytic cells is GTPase Rac [23, 24]. Correct positioning of p67phox with gp91phox depends mostly on two regulatory subunits:

p47phox and Rac1 or Rac2 [21]. Defect in activation of either one will lead to defect in NADPH oxidase activity. In our experiments we observed a decrease in activation and translocation of p47phox, however, if Rac activation was reduced as a consequence of altered Shc, it would lead to decrease in NADPH oxidase activation.

We tested activation of both Rac1 and Rac2 by fMLP and PMA. The maximal rate of Rac activation by PMA is five minutes, and one minute of fMLP treatment [25]. We found no difference in PMA-stimulated Rac1 activation between p66Shc(-/-) and wild type macrophages. A very small (1.18 times), but significant (p=0.023346) reduction in Rac1 activation was found in fMLP-stimulated mutant macrophages (Figure 8). Since p66Shc was reported to signal specifically to Rac1, and Rac1 is four times more abundant in peritoneal macrophages then Rac2 [26], we present blots measuring GTP-Rac1. GTP-Rac2 also precipitated with the PAK-1 PBD agarose conjugate and we tested GTP-Rac2 levels as well. Rac2 activation by PMA and fMLP was not different from Rac1 activation (data not shown). GTP-Rac bands have similar intensities between p66Shc(-/-) and wild type agonist-stimulated macrophages. A slight difference with fMLP stimulation was revealed only after densitometry and normalization to the loading control bands. Statistical analysis of four independent experiments with two technical replicates each (eight gels total) showed that p66Shc(-/-) macrophages have a very slightly less fMLP induced Rac1 activation, whereas PMA stimulation results in no statistically different activation of Rac in mutants and wild type macrophages.

The decrease in respiratory burst between mutant and wild type macrophages was 30-35% and was observed with fMLP, PMA and arachidonic acid stimulation. We conclude that difference in Rac activation could not explain the difference in oxidative burst between mutant and control macrophages.

p66Shc(-/-) cells have reduced phosphorylation of PrkCδ. PMA through translocation to the plasma membrane drives phosphorylation of protein kinases C (PKC) and phosphorylation of its targets. PKCδ is thought to play a central role in activation of PHOXes by phorbol esters [27]. We measured the activation of PKCδ in mutant and control macrophages induced with PMA. A western blot, representing 18 similar experiments, is shown (Figure 9 A). The primary antibodies for total PKCδ were from mouse and primary antibodies for the phospho-PKCδ were from rabbit host species. We used secondary antibody labeled with different infrared dyes as described in methods section. This creates the possibility to run total PKCδ (loading control) and phospho-PKCδ quantification on the same membrane. We measured band intensities for phospho PKCδ and total PKCδ on our Western blots. Bars on the graph presented on picture (Figure 9 B) are intensities of phospho PKC delta divided by PKC delta. Error bars are standard deviations of 18 experiments. On the Western blot (Figure 9 A), the bands corresponding to p66Shc(-/-) PMA induced phospho-PKCδ looks lighter than control ones. As shown on the bar graph, PMA-stimulated PKCδ phosphorylation in mutant macrophages was significantly reduced for about 30% comparing to control macrophages ones, p-value 0.017. In mock-treated macrophages no significant difference in phospho – PKCδ abundance in mutant macrophages versus control was observed, p – value 0.91 (Figure 9 B). Since the difference in ROS production is only 30-40%, we didn't expect a bigger defect in phosphorylation of PKC delta. Thus, the defect in NADPH oxidase activation in p66Shc(-/-) cells can be explained by a decrease in phosphorylation rate of PKCδ and, as a result, decrease in activation of p47phox.

p66Shc-/- marophages have reduced activation of Akt and ERK by fMLP. A number of kinases have been proposed to participate in p47phox phosphorylation events, among which Akt and ERK have being reported [28-30]. We tested Akt and ERK activation after one minute of fMLP treatment in mutant and control macrophages using anti-phospho Akt, anti-total Akt, anti-phospho ERK and anti-total ERK antibody. The antibodies were from different species and, it was possible to analyze phospho-specific and total antigen specific bands on the same membrane at the same time. The activation of Akt and ERK was lower in mutant macrophages (Figure 10) p=0.029532, and p=0.046206 respectively. The difference in PKC activation between p66Shc(-/-) and wild type cells in our experiments was about 30%. The difference in Akt and ERK activation was about 30% also. We suggest that since Akt and ERKs have been reported to be activators of p47Phox, decreased phosphorylation of Akt/ERK in p66Shc-deficient mice contributes to decreased activation of p47Phox.

Discussion

Long-lived 66Shc-deficient mice produce less superoxide through macrophage NADPH oxidase. p66Shc-deficient mice have an extended lifespan, and their cells produce less ROS, and are resistant to oxidative stress. We sought to identify the basis of the extended lifespan. We observe that the NADPH-dependent production of superoxide is deficient in p66Shc KO mice. The defect does not appear to result from any deficiency in PHOX protein expression but rather through a Shc-dependent defect in the signaling and phosphorylation and assembly of the PHOX complex. Resistances to oxidative stress, altered insulin sensitivity and reduced body mass have been reported for multiple mouse longevity models [31]. We suggest that reduced NADPH-oxidase dependent superoxide production could be the basis for reduced inflammatory and oxidative disease in these long-lived mutants, and could contribute to their increased lifespan.

Activation of p47phox and kinases, implicated in p47phox phosphorylation, are lower in p66Shc(-/-) mice. The deficiency in NADPH Oxidase-mediated superoxide production in mutant mice could have been the result of several p66Shc-dependent causes: deficiency in PHOX subunits or heme. However, we observed no evidence of deficiency of PHOX related proteins or heme. By contrast, the phosphorylation rate of p47phox was clearly and significantly lower in mutants compared to controls.

A number of kinases have been proposed to participate in p47phox phosphorylation events, in particular, protein kinase C (PKC), mitogen-activated protein kinases (MAPKs) [20], extracellular signal-regulated kinase (ERK1/2) [28], p21-activated kinase (PAK) [32, 33] and protein kinase B (PKB)/Akt [29, 30]. Since we did not observe a big difference between p66Shc KO and WT macrophages in activation of Rac, we do not expect activation of PAK, which is downstream of Rac. fMLP treatment of phagocytic cells leads to activation of Src related kinase Lyn [34] and Syk. Shc proteins are downstream and implicated in signaling to Akt and ERK through binding to Grb2, SOS and activation of Ras in phagocytic cells [35, 36]. Major signal conductors were reported to be p52Shc and p66Shc [37]. However, this is not the only way for activation of ERK and MAPK in hematopoietic cells [38]. In the p66Shc KO background, changes in Shc expression could affect activation of PI3K, Akt and ERK.

In our experiments we observed that level of activation of PKCδ was lower in mutants. PKCδ is critical for phosphorylation of p47phox [27, 39]. It has been shown that Shc directly interacts, co-localizes and co-translocates with PKCδ in different type of cells including MEFS [40], hematopoietic cells [41], pancreatic cells [42], COS cells [43]. Upon stress, p52Shc and especially p66Shc [43] gets phosphorylated by PKCδ, p46Shc has been shown to be similarly phosphorylated by PKCδ as p66Shc. Thus, there is clear connection of Shc proteins to PKC signaling and changes in expression of Shcs are expected to affect PKC activation rates, as we observe in p66Shc (-/-) cells.

Akt and ERK kinases are downstream of Shc proteins in signaling cascades. Thus, defect in expression of Shc would lead to defect in signaling to Akt and ERK through Shc/Grb2/SOS/Ras/PI3K pathway. In our experiments we observed such defects as decreased activation of Akt and ERK for about 30%. We propose that defect in PKCδ, Akt and ERK activation contributes to the defect in p47phox phosphorylation, and ultimately to the defect in PHOX activation and superoxide production.

Rac activation is similar in p66Shc (-/-) macrophages. Another component crucially important for efficiency of NADPH oxidase activation in phagocytic cells is GTPase Rac [23, 24]. Studies shown that p66Shc redirects the signaling of Shc through SOS toward Rac1 activation and consequently leads to ROS production in mouse embryonic fibroblasts (MEFS) in response to stress [44]. Activated Rac, in turn, has being reported to increase phosphorylation, reduce ubiquitination and stabilize p66Shc protein [45]. P67phox was reported to be effector of both Rac1 and Rac2. In macrophages mostly Rac1 is responsible for NADPH oxidase activation [46]. Moreover, binding of Rac- or Cdc42-GTP leads to PAK auto-phosphorylation and activation of the ability to phosphorylate exogenous substrates on serine and/or threonine residues. Substrates for PAK in human neutrophils may include the p47*phox* and p67*phox* - NADPH oxidase components [32, 47]. Thus, defect in Rac/PAK-1 activation would lead to defect in p47phox phosphorylation. Also, defect in Rac activation itself would lead to defect in p67phox assembly with gp91phox.

In our experiments GTP-Rac levels in p66Shc(-/-) and wild type agonist stimulated macrophages were similar. A very slight decrease with fMLP stimulation was observed. PMA simulation resulted in no significant difference in activation of Rac in mutants and wild type macrophages. However the 30-40% decrease in respiratory burst in mutant macrophages was observed with all stimulators: fMLP, PMA and arachidonic acid. We conclude that difference in Rac

activation cannotexplain the difference in oxidative burst between mutant and control macrophages.

It has been shown that p66Shc signals to Rac1 and leads to ROS production in some cell types. In our study we saw only a tiny effect of p66Shc deletion on Rac activation in peritoneal macrophages. The p66Shc level in wild type macrophages is very small and is very similar to the Shc levels in RAW-cells (Figure 7), <1% compared to the other isoforms p52 and p46 Shc. However Mouse Embryonic Fibroblasts have very high p66Shc levels, such that p66=p52=p46[45] and our data not shown. This is a potential explanation for the different results obtained in current study on macrophages and a former study employing MEFS [44].

G protein-coupled receptors, Shc and NADPH Oxidase activity. Agonists activate G protein-coupled receptors (GPCRs) - the Gi family of heterotrimeric G proteins in hematopoietic cells which are composed of Gα, Gβ, and Gγ subunits. Ligand binding to receptors catalyzes the GDP for GTP exchange on the Gα subunit, liberating it from the Gβγ complex. Free Gβ, and Gγ subunits directly bounds to downstream effectors [48] and direct functions including chemotaxis and superoxide production [49]. Thus, GPCR signals to phosphoinositide 3-kinase-γ (PI3Kγ) [50] with subsequent synthesis of phosphatidylinositol -3', 4', 5'- triphosphate (PIP_3) followed by PIP_3 activated kinase (PDK) and Akt activation. Akt is one of the activators of p47phox [29, 30]. PIP3 required for the activation of GEF – DOCK-2 and for the anchoring of p47phox and p40phox on the membrane during NADPH-oxidase assembly [51-55]. Activation of PI3K has being reported to require active Ras, which is downstream of Shcs. Shcs are activated by GPCRs through tyrosine kinases Lyn and Syk [34, 35, 56] and cause GRB2/SOS/Ras/Raf/MEK-dependent ERK activation. ERKs are activators of p47phox [28]. Active Gβγ's also activate phosphoinositide-specific phospholipase-β (PLCβ) [57, 58], which, in turn, lead to generation of inositol trisphosphate (IP3), with the consequent mobilization of Ca2+ from intracellular stores, and diacylglycerol (DAG), with the consequent activation of various protein kinase C (PKC) isoforms, including DAG-sensitive calcium dependent kinase-PKCδ. It have being demonstrated that PKCδ, on one hand directly interacts with Shc [40-43]. Also, PKCδ is an activator of p47phox [27, 39, 59, 60].

Thus, activations of PKCδ, Akt and ERKs are dependent on activation and expression of Shcs. On another arm of the pathway, GPCR signals to GTP Exchange Factor (GEF) – Vav through the Src Family kinases Hck and Fgr and cause GDP-GTP exchange and activation of Rac GTP-ase, leading to Rac translocation and participation on NADPH-oxidase assembly [58]. Also, activated Rac signal to PAK-1, which has been reported to be a p47phox, a NADPH-oxidase regulatory subunit, activator [32, 33]. One more way in which GPCR activates Rac is through the direct activation of GEF–P-Rex by the free Gβγ [61], however, this requires PIP3. Thus, Rac activation could has the potential bypass the Shc-dependent pathways (Figure 11).

So, we observe a Shc-dependent defect in activation of PKCδ, Akt and ERK with consequent effect on activation of p47phox, consistent with defective activation of the right and center arms of the pathway descending from Gi stimulation. We only observe a very slight decrease in GTP-Rac binding (the left arm and non-Shc dependent part of the pathway), and this defect is not sufficient to explain the 30-40% decrease in NADPH Oxidase-dependent superoxide production.

Potential consequences of NADPH-oxidase deficiency in p66Shc(-/-) mice. Reduced ROS production and resistance to oxidative stress has also been reported to extend lifespan in several invertebrate model systems [62-67]. Resistance to oxidative stress, altered insulin sensitivity and reduced body mass has been reported for multiple mouse longevity models [31]. However the support for longevity as a result of increased protection from oxidative stress in rodents is mixed. While CuZnSOD and MnSOD deficiency cause increased ROS *in vivo* and shortened lifespan [68, 69], overexpression of CuZnSOD and MnSOD does not appear to extend mouse lifespan [70-72]. However, increased mitochondrial catalase expression has been reported to increase lifespan and healthspan in mice [73, 74], and increased CuZnSOD in rats increases lifespan (Richardson, personal communication).

p66Shc-deficient mice have been observed to be resistant to several types of age-related pathology associated with oxidative stress and/or inflammation (which can be caused by phagocytic cells), including vascular disease [5], age related endothelial dysfunction [75], oxidative inflammatory kidney damage [8, 76], hyperglycemia-induced endothelial dysfunction and oxidative stress [7], and brain oxidative stress [77]. This resistance could be the result of decreased oxidative stress, or decreased inflammatory response. Two major sources of cellular ROS production are NADPH Oxidase (PHOX) and mitochondria. A small decrease in CCL4-dependent

mitochondrial ROS generation was shown previously for p66ShcKO mice [4]; however, PHOX- dependent superoxide production has not been investigated.

We observe that the NADPH-dependent production of superoxide is deficient in p66Shc mice. The defect does not appear to result from any deficiency in PHOX protein expression but rather through a Shc-dependent defect in the signaling and phosphorylation and assembly of the PHOX complex. This defect in PHOX-dependent superoxide generation has the potential to explain the reported resistance of p66Shc knockout mice to oxidative pathologies in endothelial cells, kidney and brain, and could also underlie the relative sensitivity of p66Shc mice to insulin and their longevity. Further studies are necessary to clarify the role of reduced oxidative stress in longevity.

In the present work we demonstrate that ROS production by NADPH-oxidase is deficient in p66Shc knockouts. We suggest that reduced NADPH-oxidase dependent superoxide production could be the basis for reduced inflammatory and oxidative disease in these long-lived mutants. Activation of NADPH oxidase and inflammation is perhaps the most clear example of antagonistic pleiotropy [78], i.e. an increase in ROS production is protective at a young age but causes multiple age related pathologies, including atherosclerosis, hypertension, nephropathy rheumatoid arthritis, [79]. An increase in several markers of inflammation with age is observed in many species including human, and is thought to cause lifespan-limiting pathology, in inflammatory hypotheses of aging [80-83] with special emphasis on phagocytic cells [84]. Multiple anti-inflammatory changes occur in long-lived Ames dwarf mice [85]. Dietary restriction appears to decrease inflammation and it is thought that this is one mechanism by which it increases lifespan [86]. Anti-inflammatory drugs can block age-related pathology, neuro-degeneration and extend lifespan in several species, including mice [87-90] and drosophila [91]. We suggest that reduced NADPH oxidase activity could contribute to reduced inflammation in p66Shc KO mice and underlie their increased lifespan.

Acknowledgements.

This work was supported by USPHS AG025532, AG16719, EY12245. We thank H Forman for advice with assays.

References

1.Harman, D., *Aging: a theory based on free radical and radiation chemistry.* J Gerontol, 1956. **11**(3): p. 298-300.

2.Migliaccio, E., M. Giorgio, S. Mele, G. Pelicci, P. Reboldi, P.P. Pandolfi, L. Lanfrancone, and P.G. Pelicci, *The p66shc adaptor protein controls oxidative stress response and life span in mammals.* Nature, 1999. **402**(6759): p. 309-13.

3.Berniakovich, I., M. Trinei, M. Stendardo, E. Migliaccio, S. Minucci, P. Bernardi, P.G. Pelicci, and M. Giorgio, *p66Shc-generated oxidative signal promotes fat accumulation*. 2008. p. M804362200.

4.Giorgio, M., E. Migliaccio, F. Orsini, D. Paolucci, M. Moroni, C. Contursi, G. Pelliccia, L. Luzi, S. Minucci, M. Marcaccio, P. Pinton, R. Rizzuto, P. Bernardi, F. Paolucci, and P.G. Pelicci, *Electron transfer between cytochrome c and p66Shc generates reactive oxygen species that trigger mitochondrial apoptosis.* Cell, 2005. **122**(2): p. 221-33.

5.Napoli, C., I. Martin-Padura, F. de Nigris, M. Giorgio, G. Mansueto, P. Somma, M. Condorelli, G. Sica, G. De Rosa, and P. Pelicci, *Deletion of the p66Shc longevity gene reduces systemic and tissue oxidative stress, vascular cell apoptosis, and early atherogenesis in mice fed a high-fat diet.* Proc Natl Acad Sci U S A, 2003. **100**(4): p. 2112-6.

6.Martin-Padura, I., F. de Nigris, E. Migliaccio, G. Mansueto, S. Minardi, M. Rienzo, L.O. Lerman, M. Stendardo, M. Giorgio, G. De Rosa, P.G. Pelicci, and C. Napoli, *p66Shc deletion confers vascular protection in advanced atherosclerosis in hypercholesterolemic apolipoprotein E knockout mice.* Endothelium, 2008. **15**(5-6): p. 276-87.

7.Camici, G.G., M. Schiavoni, P. Francia, M. Bachschmid, I. Martin-Padura, M. Hersberger, F.C. Tanner, P. Pelicci, M. Volpe, P. Anversa, T.F. Luscher, and F. Cosentino, *Genetic deletion of p66(Shc) adaptor protein prevents hyperglycemia-induced endothelial dysfunction and oxidative stress.* Proc Natl Acad Sci U S A, 2007. **104**(12): p. 5217-22.

8.Menini, S., C. Iacobini, C. Ricci, G. Oddi, C. Pesce, F. Pugliese, K. Block, H.E. Abboud, M. Giorgio, E. Migliaccio, P.G. Pelicci, and G. Pugliese, *Ablation of the gene encoding p66Shc protects mice against AGE-induced glomerulopathy by preventing oxidant-dependent tissue injury and further AGE accumulation.* Diabetologia, 2007. **50**(9): p. 1997-2007.

9.Kisielow, M., S. Kleiner, M. Nagasawa, A. Faisal, and Y. Nagamine, *Isoform-specific knockdown and expression of adaptor protein ShcA using small interfering RNA.* Biochem J, 2002. **363**(Pt 1): p. 1-5.

10.Schadt, E.E., C. Li, B. Ellis, and W.H. Wong, *Feature extraction and normalization algorithms for high-density oligonucleotide gene expression array data.* J Cell Biochem Suppl, 2001. **Suppl 37**: p. 120-5.

11.Khatri, P., P. Bhavsar, G. Bawa, and S. Draghici, *Onto-Tools: an ensemble of web-accessible, ontology-based tools for the functional design and interpretation of high-throughput gene expression experiments.* Nucleic Acids Res, 2004. **32**(Web Server issue): p. W449-56.

12.Draghici, S., P. Khatri, A.L. Tarca, K. Amin, A. Done, C. Voichita, C. Georgescu, and R. Romero, *A systems biology approach for pathway level analysis.* Genome Res, 2007. **17**(10): p. 1537-45.

13.Hancock, J.T. and O.T. Jones, *The inhibition by diphenyleneiodonium and its analogues of superoxide generation by macrophages.* Biochem J, 1987. **242**(1): p. 103-7.

14.Nishida, S., L.S. Yoshida, T. Shimoyama, H. Nunoi, T. Kobayashi, and S. Tsunawaki, *Fungal metabolite gliotoxin targets flavocytochrome b558 in the activation of the human neutrophil NADPH oxidase.* Infect Immun, 2005. **73**(1): p. 235-44.

15.Tsunawaki, S., L.S. Yoshida, S. Nishida, T. Kobayashi, and T. Shimoyama, *Fungal metabolite gliotoxin inhibits assembly of the human respiratory burst NADPH oxidase.* Infect Immun, 2004. **72**(6): p. 3373-82.

16.Yoshida, L.S., S. Abe, and S. Tsunawaki, *Fungal gliotoxin targets the onset of superoxide-generating NADPH oxidase of human neutrophils.* Biochem Biophys Res Commun, 2000. **268**(3): p. 716-23.

17.Datla, S.R., G.J. Dusting, T.A. Mori, C.J. Taylor, K.D. Croft, and F. Jiang, *Induction of heme oxygenase-1 in vivo suppresses NADPH oxidase derived oxidative stress.* Hypertension, 2007. **50**(4): p. 636-42.

18.Taille, C., J. El-Benna, S. Lanone, M.C. Dang, E. Ogier-Denis, M. Aubier, and J. Boczkowski, *Induction of heme oxygenase-1 inhibits NAD(P)H oxidase activity by down-regulating cytochrome b558 expression via the reduction of heme availability.* J Biol Chem, 2004. **279**(27): p. 28681-8.
19.Durand, D., D. Cannella, V. Dubosclard, E. Pebay-Peyroula, P. Vachette, and F. Fieschi, *Small-angle X-ray scattering reveals an extended organization for the autoinhibitory resting state of the p47(phox) modular protein.* Biochemistry, 2006. **45**(23): p. 7185-93.
20.El Benna, J., R.P. Faust, J.L. Johnson, and B.M. Babior, *Phosphorylation of the respiratory burst oxidase subunit p47phox as determined by two-dimensional phosphopeptide mapping. Phosphorylation by protein kinase C, protein kinase A, and a mitogen-activated protein kinase.* J Biol Chem, 1996. **271**(11): p. 6374-8.
21.Leusen, J.H., A.J. Verhoeven, and D. Roos, *Interactions between the components of the human NADPH oxidase: a review about the intrigues in the phox family.* Front Biosci, 1996. **1**: p. d72-90.
22.Okamura, N., S.E. Malawista, R.L. Roberts, H. Rosen, H.D. Ochs, B.M. Babior, and J.T. Curnutte, *Phosphorylation of the oxidase-related 48K phosphoprotein family in the unusual autosomal cytochrome-negative and X-linked cytochrome-positive types of chronic granulomatous disease*. 1988. p. 811-816.
23.Abo, A., E. Pick, A. Hall, N. Totty, C.G. Teahan, and A.W. Segal, *Activation of the NADPH oxidase involves the small GTP-binding protein p21rac1.* Nature, 1991. **353**(6345): p. 668-70.
24.Knaus, U.G., P.G. Heyworth, T. Evans, J.T. Curnutte, and G.M. Bokoch, *Regulation of phagocyte oxygen radical production by the GTP-binding protein Rac 2.* Science, 1991. **254**(5037): p. 1512-5.
25.Benard, V., B.P. Bohl, and G.M. Bokoch, *Characterization of rac and cdc42 activation in chemoattractant-stimulated human neutrophils using a novel assay for active GTPases.* J Biol Chem, 1999. **274**(19): p. 13198-204.
26.Yamauchi, A., C. Kim, S. Li, C.C. Marchal, J. Towe, S.J. Atkinson, and M.C. Dinauer, *Rac2-deficient murine macrophages have selective defects in superoxide production and phagocytosis of opsonized particles.* J Immunol, 2004. **173**(10): p. 5971-9.
27.Bankers-Fulbright, J.L., H. Kita, G.J. Gleich, and S.M. O'Grady, *Regulation of human eosinophil NADPH oxidase activity: a central role for PKCdelta.* J Cell Physiol, 2001. **189**(3): p. 306-15.
28.Dewas, C., M. Fay, M.A. Gougerot-Pocidalo, and J. El-Benna, *The mitogen-activated protein kinase extracellular signal-regulated kinase 1/2 pathway is involved in formyl-methionyl-leucyl-phenylalanine-induced p47phox phosphorylation in human neutrophils.* J Immunol, 2000. **165**(9): p. 5238-44.
29.Didichenko, S.A., B. Tilton, B.A. Hemmings, K. Ballmer-Hofer, and M. Thelen, *Constitutive activation of protein kinase B and phosphorylation of p47phox by a membrane-targeted phosphoinositide 3-kinase.* Curr Biol, 1996. **6**(10): p. 1271-8.
30.Chen, Q., D.W. Powell, M.J. Rane, S. Singh, W. Butt, J.B. Klein, and K.R. McLeish, *Akt phosphorylates p47phox and mediates respiratory burst activity in human neutrophils.* J Immunol, 2003. **170**(10): p. 5302-8.
31.Bartke, A., *New findings in gene knockout, mutant and transgenic mice.* Exp Gerontol, 2008. **43**(1): p. 11-4.
32.Knaus, U.G., S. Morris, H.J. Dong, J. Chernoff, and G.M. Bokoch, *Regulation of human leukocyte p21-activated kinases through G protein--coupled receptors.* Science, 1995. **269**(5221): p. 221-3.
33.Martyn, K.D., M.J. Kim, M.T. Quinn, M.C. Dinauer, and U.G. Knaus, *p21-activated kinase (Pak) regulates NADPH oxidase activation in human neutrophils.* Blood, 2005. **106**(12): p. 3962-9.
34.Hibbs, M.L. and A.R. Dunn, *Lyn, a src-like tyrosine kinase.* Int J Biochem Cell Biol, 1997. **29**(3): p. 397-400.
35.Ptasznik, A., A. Traynor-Kaplan, and G.M. Bokoch, *G protein-coupled chemoattractant receptors regulate Lyn tyrosine kinase.Shc adapter protein signaling complexes.* J Biol Chem, 1995. **270**(34): p. 19969-73.

36.Erdreich-Epstein, A., M. Liu, A.M. Kant, K.D. Izadi, J.A. Nolta, and D.L. Durden, *Cbl functions downstream of Src kinases in Fc gamma RI signaling in primary human macrophages.* J Leukoc Biol, 1999. **65**(4): p. 523-34.
37.Miura, K. and D.W. MacGlashan, *Phosphatidylinositol-3 kinase regulates p21ras activation during IgE-mediated stimulation of human basophils.* Blood, 2000. **96**(6): p. 2199-205.
38.Torres, M. and R.D. Ye, *Activation of the mitogen-activated protein kinase pathway by fMet-leu-Phe in the absence of Lyn and tyrosine phosphorylation of SHC in transfected cells.* J Biol Chem, 1996. **271**(22): p. 13244-9.
39.Cheng, N., R. He, J. Tian, M.C. Dinauer, and R.D. Ye, *A critical role of protein kinase C delta activation loop phosphorylation in formyl-methionyl-leucyl-phenylalanine-induced phosphorylation of p47(phox) and rapid activation of nicotinamide adenine dinucleotide phosphate oxidase.* J Immunol, 2007. **179**(11): p. 7720-8.
40.Hu, Y., C. Kang, R.J. Philp, and B. Li, *PKC delta phosphorylates p52ShcA at Ser29 to regulate ERK activation in response to H2O2.* Cell Signal, 2007. **19**(2): p. 410-8.
41.Leitges, M., K. Gimborn, W. Elis, J. Kalesnikoff, M.R. Hughes, G. Krystal, and M. Huber, *Protein kinase C-delta is a negative regulator of antigen-induced mast cell degranulation.* Mol Cell Biol, 2002. **22**(12): p. 3970-80.
42.Pace, A., J.A. Tapia, L.J. Garcia-Marin, and R.T. Jensen, *The Src family kinase, Lyn, is activated in pancreatic acinar cells by gastrointestinal hormones/neurotransmitters and growth factors which stimulate its association with numerous other signaling molecules.* Biochim Biophys Acta, 2006. **1763**(4): p. 356-65.
43.Morita, M., H. Matsuzaki, T. Yamamoto, Y. Fukami, and U. Kikkawa, *Epidermal growth factor receptor phosphorylates protein kinase C {delta} at Tyr332 to form a trimeric complex with p66Shc in the H2O2-stimulated cells.* J Biochem, 2008. **143**(1): p. 31-8.
44.Khanday, F.A., L. Santhanam, K. Kasuno, T. Yamamori, A. Naqvi, J. DeRicco, A. Bugayenko, I. Mattagajasingh, A. Disanza, G. Scita, and K. Irani, *Sos-mediated activation of rac1 by p66shc*. 2006. p. 817-822.
45.Khanday, F.A., T. Yamamori, I. Mattagajasingh, Z. Zhang, A. Bugayenko, A. Naqvi, L. Santhanam, N. Nabi, K. Kasuno, B.W. Day, and K. Irani, *Rac1 Leads to Phosphorylation-dependent Increase in Stability of the p66shc Adaptor Protein: Role in Rac1-induced Oxidative Stress.* Mol. Biol. Cell, 2006. **17**(1): p. 122-129.
46.Bokoch, G.M., *Regulation of the phagocyte respiratory burst by small GTP-binding proteins.* Trends Cell Biol, 1995. **5**(3): p. 109-13.
47.Ahmed, S., E. Prigmore, S. Govind, C. Veryard, R. Kozma, F.B. Wientjes, A.W. Segal, and L. Lim, *Cryptic Rac-binding and p21(Cdc42Hs/Rac)-activated kinase phosphorylation sites of NADPH oxidase component p67(phox).* J Biol Chem, 1998. **273**(25): p. 15693-701.
48.Oldham, W.M. and H.E. Hamm, *Structural basis of function in heterotrimeric G proteins.* Q Rev Biophys, 2006. **39**(2): p. 117-66.
49.Neptune, E.R. and H.R. Bourne, *Receptors induce chemotaxis by releasing the betagamma subunit of Gi, not by activating Gq or Gs.* Proc Natl Acad Sci U S A, 1997. **94**(26): p. 14489-94.
50.Stoyanov, B., S. Volinia, T. Hanck, I. Rubio, M. Loubtchenkov, D. Malek, S. Stoyanova, B. Vanhaesebroeck, R. Dhand, B. Nurnberg, and et al., *Cloning and characterization of a G protein-activated human phosphoinositide-3 kinase.* Science, 1995. **269**(5224): p. 690-3.
51.Bissonnette, S.A., C.M. Glazier, M.Q. Stewart, G.E. Brown, C.D. Ellson, and M.B. Yaffe, *Phosphatidylinositol 3-phosphate-dependent and -independent functions of p40phox in activation of the neutrophil NADPH oxidase.* J Biol Chem, 2008. **283**(4): p. 2108-19.
52.Ellson, C., K. Davidson, K. Anderson, L.R. Stephens, and P.T. Hawkins, *PtdIns3P binding to the PX domain of p40phox is a physiological signal in NADPH oxidase activation.* Embo J, 2006. **25**(19): p. 4468-78.

53.Zhan, Y., J.V. Virbasius, X. Song, D.P. Pomerleau, and G.W. Zhou, *The p40phox and p47phox PX domains of NADPH oxidase target cell membranes via direct and indirect recruitment by phosphoinositides.* J Biol Chem, 2002. **277**(6): p. 4512-8.
54.Wientjes, F.B., E.P. Reeves, V. Soskic, H. Furthmayr, and A.W. Segal, *The NADPH oxidase components p47(phox) and p40(phox) bind to moesin through their PX domain.* Biochem Biophys Res Commun, 2001. **289**(2): p. 382-8.
55.Stahelin, R.V., A. Burian, K.S. Bruzik, D. Murray, and W. Cho, *Membrane binding mechanisms of the PX domains of NADPH oxidase p40phox and p47phox.* J Biol Chem, 2003. **278**(16): p. 14469-79.
56.Hibbs, M.L., K.W. Harder, J. Armes, N. Kountouri, C. Quilici, F. Casagranda, A.R. Dunn, and D.M. Tarlinton, *Sustained activation of Lyn tyrosine kinase in vivo leads to autoimmunity.* J Exp Med, 2002. **196**(12): p. 1593-604.
57.Li, Z., H. Jiang, W. Xie, Z. Zhang, A.V. Smrcka, and D. Wu, *Roles of PLC-beta2 and -beta3 and PI3Kgamma in chemoattractant-mediated signal transduction.* Science, 2000. **287**(5455): p. 1046-9.
58.Fumagalli, L., H. Zhang, A. Baruzzi, C.A. Lowell, and G. Berton, *The Src family kinases Hck and Fgr regulate neutrophil responses to N-formyl-methionyl-leucyl-phenylalanine.* J Immunol, 2007. **178**(6): p. 3874-85.
59.Remijsen, Q.F., A. Fontayne, F. Verdonck, E. Clynen, L. Schoofs, and J. Willems, *The antimicrobial peptide parabutoporin competes with p47(phox) as a PKC-substrate and inhibits NADPH oxidase in human neutrophils.* FEBS Lett, 2006. **580**(26): p. 6206-10.
60.Nauseef, W.M., B.D. Volpp, S. McCormick, K.G. Leidal, and R.A. Clark, *Assembly of the neutrophil respiratory burst oxidase. Protein kinase C promotes cytoskeletal and membrane association of cytosolic oxidase components.* J Biol Chem, 1991. **266**(9): p. 5911-7.
61.Welch, H.C., W.J. Coadwell, C.D. Ellson, G.J. Ferguson, S.R. Andrews, H. Erdjument-Bromage, P. Tempst, P.T. Hawkins, and L.R. Stephens, *P-Rex1, a PtdIns(3,4,5)P3- and Gbetagamma-regulated guanine-nucleotide exchange factor for Rac.* Cell, 2002. **108**(6): p. 809-21.
62.Orr, W.C. and R.S. Sohal, *Extension of life-span by overexpression of superoxide dismutase and catalase in Drosophila melanogaster.* Science, 1994. **263**(5150): p. 1128-30.
63.Sohal, R.S. and R. Weindruch, *Oxidative stress, caloric restriction, and aging.* Science, 1996. **273**(5271): p. 59-63.
64.Murakami, S., *Stress resistance in long-lived mouse models.* Exp Gerontol, 2006. **41**(10): p. 1014-9.
65.Radyuk, S.N., K. Michalak, V.I. Klichko, J. Benes, I. Rebrin, R.S. Sohal, and W.C. Orr, *Peroxiredoxin 5 confers protection against oxidative stress and apoptosis and also promotes longevity in Drosophila.* Biochem J, 2009. **419**(2): p. 437-45.
66.Legan, S.K., I. Rebrin, R.J. Mockett, S.N. Radyuk, V.I. Klichko, R.S. Sohal, and W.C. Orr, *Overexpression of glucose-6-phosphate dehydrogenase extends the life span of Drosophila melanogaster.* J Biol Chem, 2008. **283**(47): p. 32492-9.
67.Luchak, J.M., L. Prabhudesai, R.S. Sohal, S.N. Radyuk, and W.C. Orr, *Modulating longevity in Drosophila by over- and underexpression of glutamate-cysteine ligase.* Ann N Y Acad Sci, 2007. **1119**: p. 260-73.
68.Huang, T.T., E.J. Carlson, H.M. Kozy, S. Mantha, S.I. Goodman, P.C. Ursell, and C.J. Epstein, *Genetic modification of prenatal lethality and dilated cardiomyopathy in Mn superoxide dismutase mutant mice.* Free Radic Biol Med, 2001. **31**(9): p. 1101-10.
69.Li, Y., T.T. Huang, E.J. Carlson, S. Melov, P.C. Ursell, J.L. Olson, L.J. Noble, M.P. Yoshimura, C. Berger, P.H. Chan, D.C. Wallace, and C.J. Epstein, *Dilated cardiomyopathy and neonatal lethality in mutant mice lacking manganese superoxide dismutase.* Nat Genet, 1995. **11**(4): p. 376-81.
70.Perez, V.I., H. Van Remmen, A. Bokov, C.J. Epstein, J. Vijg, and A. Richardson, *The overexpression of major antioxidant enzymes does not extend the lifespan of mice.* Aging Cell, 2009. **8**(1): p. 73-5.
71.Van Remmen, H., Y. Ikeno, M. Hamilton, M. Pahlavani, N. Wolf, S.R. Thorpe, N.L. Alderson, J.W. Baynes, C.J. Epstein, T.T. Huang, J. Nelson, R. Strong, and A. Richardson, *Life-long reduction in*

MnSOD activity results in increased DNA damage and higher incidence of cancer but does not accelerate aging. Physiol Genomics, 2003. **16**(1): p. 29-37.
72.Mele, J., H. Van Remmen, J. Vijg, and A. Richardson, *Characterization of transgenic mice that overexpress both copper zinc superoxide dismutase and catalase.* Antioxid Redox Signal, 2006. **8**(3-4): p. 628-38.
73.Schriner, S.E., N.J. Linford, G.M. Martin, P. Treuting, C.E. Ogburn, M. Emond, P.E. Coskun, W. Ladiges, N. Wolf, H. Van Remmen, D.C. Wallace, and P.S. Rabinovitch, *Extension of murine life span by overexpression of catalase targeted to mitochondria.* Science, 2005. **308**(5730): p. 1909-11.
74.Treuting, P.M., N.J. Linford, S.E. Knoblaugh, M.J. Emond, J.F. Morton, G.M. Martin, P.S. Rabinovitch, and W.C. Ladiges, *Reduction of age-associated pathology in old mice by overexpression of catalase in mitochondria.* J Gerontol A Biol Sci Med Sci, 2008. **63**(8): p. 813-22.
75.Francia, P., C. delli Gatti, M. Bachschmid, I. Martin-Padura, C. Savoia, E. Migliaccio, P.G. Pelicci, M. Schiavoni, T.F. Luscher, M. Volpe, and F. Cosentino, *Deletion of p66shc gene protects against age-related endothelial dysfunction.* Circulation, 2004. **110**(18): p. 2889-95.
76.Menini, S., L. Amadio, G. Oddi, C. Ricci, C. Pesce, F. Pugliese, M. Giorgio, E. Migliaccio, P. Pelicci, C. Iacobini, and G. Pugliese, *Deletion of p66Shc longevity gene protects against experimental diabetic glomerulopathy by preventing diabetes-induced oxidative stress.* Diabetes, 2006. **55**(6): p. 1642-50.
77.Berry, A., A. Greco, M. Giorgio, P.G. Pelicci, R. de Kloet, E. Alleva, L. Minghetti, and F. Cirulli, *Deletion of the lifespan determinant p66(Shc) improves performance in a spatial memory task, decreases levels of oxidative stress markers in the hippocampus and increases levels of the neurotrophin BDNF in adult mice.* Exp Gerontol, 2008. **43**(3): p. 200-208.
78.Caruso, C., D. Lio, L. Cavallone, and C. Franceschi, *Aging, longevity, inflammation, and cancer.* Ann N Y Acad Sci, 2004. **1028**: p. 1-13.
79.Lambeth, J.D., *Nox enzymes, ROS, and chronic disease: an example of antagonistic pleiotropy.* Free Radic Biol Med, 2007. **43**(3): p. 332-47.
80.Finch, C.E. and E.M. Crimmins, *Inflammatory exposure and historical changes in human life-spans.* Science, 2004. **305**(5691): p. 1736-9.
81.Gurven, M., H. Kaplan, J. Winking, C. Finch, and E.M. Crimmins, *Aging and inflammation in two epidemiological worlds.* J Gerontol A Biol Sci Med Sci, 2008. **63**(2): p. 196-9.
82.Franceschi, C., F. Olivieri, F. Marchegiani, M. Cardelli, L. Cavallone, M. Capri, S. Salvioli, S. Valensin, G. De Benedictis, A. Di Iorio, C. Caruso, G. Paolisso, and D. Monti, *Genes involved in immune response/inflammation, IGF1/insulin pathway and response to oxidative stress play a major role in the genetics of human longevity: the lesson of centenarians.* Mech Ageing Dev, 2005. **126**(2): p. 351-61.
83.Ostan, R., L. Bucci, M. Capri, S. Salvioli, M. Scurti, E. Pini, D. Monti, and C. Franceschi, *Immunosenescence and immunogenetics of human longevity.* Neuroimmunomodulation, 2008. **15**(4-6): p. 224-40.
84.Finch, C.E., *Developmental origins of aging in brain and blood vessels: an overview.* Neurobiol Aging, 2005. **26**(3): p. 281-91.
85.Dhahbi, J., X. Li, T. Tran, M.M. Masternak, and A. Bartke, *Circulating blood leukocyte gene expression profiles: effects of the Ames dwarf mutation on pathways related to immunity and inflammation.* Exp Gerontol, 2007. **42**(8): p. 772-88.
86.Morgan, T.E., A.M. Wong, and C.E. Finch, *Anti-inflammatory mechanisms of dietary restriction in slowing aging processes.* Interdiscip Top Gerontol, 2007. **35**: p. 83-97.
87.Carla, Z., C. Federica, C. Sara, C. Daniela, R. Daniela, A.C. Regiane, R. Giuseppe, and B. Ariela, *Cyclin-dependent kinase inhibition limits glomerulonephritis and extends lifespan of mice with systemic lupus.* Arthritis & Rheumatism, 2007. **56**(5): p. 1629-1637.
88.Kiaei, M., K. Kipiani, S. Petri, J. Chen, N.Y. Calingasan, and M.F. Beal, *Celastrol blocks neuronal cell death and extends life in transgenic mouse model of amyotrophic lateral sclerosis.* Neurodegener Dis, 2005. **2**(5): p. 246-54.

89.Kiaei, M., K. Kipiani, J. Chen, N.Y. Calingasan, and M.F. Beal, *Peroxisome proliferator-activated receptor-gamma agonist extends survival in transgenic mouse model of amyotrophic lateral sclerosis.* Exp Neurol, 2005. **191**(2): p. 331-6.
90.Kiaei, M., S. Petri, K. Kipiani, G. Gardian, D.K. Choi, J. Chen, N.Y. Calingasan, P. Schafer, G.W. Muller, C. Stewart, K. Hensley, and M.F. Beal, *Thalidomide and lenalidomide extend survival in a transgenic mouse model of amyotrophic lateral sclerosis.* J Neurosci, 2006. **26**(9): p. 2467-73.
91.Sykiotis, G.P. and D. Bohmann, *Keap1/Nrf2 signaling regulates oxidative stress tolerance and lifespan in Drosophila.* Dev Cell, 2008. **14**(1): p. 76-85.

Figure legends.

Table 1. Genomic effects of p66Shc knock out. Lists of top significant up or down-regulated genes through p66Shc -/- mice tissues: Spleen, Retroperitoneal fat, Liver, Lungs, Peritoneal macrophages, Epididymal fat, at both ages of 3 month and 12 month were submitted to "OntoExpress", as described in methods. Outputs of "Pathway analysis tool" and "Bioprocess analysis tool" were truncated to top most significant fore in each category and presented in the table format.

Figure 1. Six hundred thousand peritoneal macrophages pre-incubated or not, as indicated, with gliotoxin were resuspended in KRP media, containing H2HFF-BSA dye according to dye manufacturer instructions. Initial readings at excitation 480 nm and emission 520 nm were taken during first 12 minutes. PMA was added at point shown by arrow, and readings were taken during next 30 minutes. Error bars are standard error, N=2.

Figure 2. NAD(P)H oxidase activity in Peritoneal Macrophages from control and p66Shc(-/-) mice. *A.* Superoxide generation by PMA – induced peritoneal macrophages from p66Shc(-/-) and control mice, as indicated, was assayed using SOD – inhibitable cytochrome – c reduction assay. Bars represent mean amount of superoxide (pMol) per minute per 600 thousands cells. Error bars are standard deviations. N=12. *B.* Superoxide generation by PMA – induced peritoneal macrophages from p66Shc(-/-) and control mice, as indicated, was assayed using H_2HFF fluorescent dye oxidation method. Bars represents mean of slopes of fluorescence increase (excitation 480 nm, emission 530 nm) after PMA induction of macrophages. Non-induced cells were used as the baseline. *C.* Superoxide generation by fMLP – induced peritoneal macrophages from p66Shc(-/-) and control mice, as indicated, was assayed using H_2HFF fluorescent dye oxidation method. *D.* Superoxide generation by AA – induced peritoneal macrophages from p66Shc(-/-) and control mice, as indicated, was assayed using H_2HFF fluorescent dye oxidation method. Error bars are standard deviations. For H_2HFF dye oxidation method N=4.

Figure 3. Total protein was extracted from mouse peritoneal macrophages of control and p66Shc(-/-) mice, mock – treated or treated with PMA, or pretreated with gliotoxin and treated with PMA, as indicated. Blots were probed with Rabbit polyclonal antibody to p40phox, p47phox, p67phox and gp91phox. At the same time blots were probed with Mouse anti – actin beta. Bands of the NAD(P)H – oxidase components and beta actin are indicated.

Figure 4. Heme levels in blood of p66Shc(-/-) mice and control mice. Bars represents total heme presented as percent (g) in blood of fore p66Shc(-/-) and fore Control mice; two p66Shc(-/-) and Controls was at ages of 3 month and two – 12 month. Error bars are standard deviations. N=4.

Figure 5. p66Shc(-/-) cells have reduced phosphorylation of p47phox. Total protein was isolated from control or p66Shc(-/-) macrophages induced with DMSO (Mock treatment) or PMA for 5 minutes, as indicated. Samples were isoelectrofocused at pH range of 4 – 9. Isoelectrofocusing gels were transferred on top of SDS – PAGE for second dimension. Blots were probed with Goat anti – p47phox antibody. Phosphorylated (1, 2, 3, 4) and Non-phosphorylated (0) forms of p47phox are indicated. *B.* Bars represent densitometry results for the levels of Phosphorylated p47phox expressed as part of total amounts of p47phox, N=2.

Figure 6. p66Shc(-/-) macrophages have defect in translocation of p47phox to membrane upon PMA induction. *A.* Total protein was isolated from control or p66Shc(-/-) macrophages induced with DMSO (mock treatment) or PMA for 5 minutes, as indicated. Samples were cleaned from unbroken cells by centrifugation and than were separated on membrane and cytosolic fraction by ultracentrifugation at 100.000 X g. as described in methods section. Cytosolic and membrane fractions were then resolved on SDS PAGE and transferred to nitrocellulose membrane. Membrane was cut by 35 kD marker band and upper part was probed with goat anti p47phox polyclonal antibody and mouse anti actin beta primary antibodies. Lower part was probed with anti MnSOD primary antibody. Western Blot image of one out of five experiments is presented. *B.* Bars on the graf represent means of fluorescence intensities of p47phox bands from membrane fraction divided to fluorescence levels of actin beta bands. Error bars are standard deviations, N=5.

Figure 7. p66Shc(-/-) macrophages have reduced phosphorylation rate of PrkCδ. *A.* Western blots of control or p66Shc(-/-) peritoneal macrophages DMSO (Mock treated) or PMA - treated, as indicated, were probed with rabbit anti prkCd and rabbit anti phospho-prkCd antibody. Bands of prkCd and phospho-prkCd are indicated. *B.* Bars represent densitometry result for the blot, and are the levels of phospho-prkCd normalized to total prkCd. N=18, p-value = 1.7E-02

Figure 8. Mouse macrophage cell line RAW 264 with siRNA mediated p66Shc knock down have defect in NAD(P)H-oxidase dependent superoxide generation. *A.* Isoform specific siRNA mediated Knock Down of p66Shc in RAW264 cells. Total protein was extracted 48 hours after transfection with p66Shc siRNA or Control siRNA, as indicated. Blot was probed with Rabbit polyclonal anti-ShcA antibody. *B.* Bars represent the amount of p66Shc as percent of all three Shc isoforms. *C.* QRTPCR results of p66Shc expression measures normalized to beta actin levels, N=25. *D.* NAD(P)H-oxidase activity in p66Shc KD and control RAW264 cells. Bars represent the means of slopes of fluorescence increase of H_2HFF dye after PMA induction. Non-PMA induced cells were used as baseline. Error bars are standard deviations, N=25.

Figure 9. *p66Shc(-/-) macrophages do not have a big defect in Rac1/2 activation. A.* Precipitates of Rac1/2 were prepared from PMA and Mock treated macrophages of p66Shc(-/-) and Control mice as described in methods section, resolved by SDS PAGE, and blots were probed with mouse monoclonal anti-Rac1 primary antibody. Presented is one of three independent blots. Rac1 and loading control bands, "mock treated", PMA treated (five minutes 3 μg/ml) samples and GTPγS loaded samples are indicated. *B.* Similar experiments as on panel *A,* but performed with 60 seconds 10 μM fMLP stimulation. *C.* Bars represent levels of GTP-Rac1 normalized by loading control band. Between experiments normalization was performed using experimental mean of each experiment. Error bars are SE, N=3. *D.* Similar to panel *C.* but experiments performed with fMLP stimulation. N=8.

Figure 10. *p66Shc(-/-) macrophages have lower fMLP induced Akt activation. A.* Macrophages from mutant and control mice were induced with fMLP as described above, reaction was stopped by dilution 5 times with ice cold PBS and cells were lysed with ice cold lysis buffer as for the Rac activation assay. Western blot was hybridized with mouse anti-phospho Akt and with rabbit anti-total Akt antibody at the same time and developed using Licor imaging system as described above. *B.* Bands corresponding to phospho Akt and total Akt were quantified, and intensities of phospho Akt bands were divided by intensities of total Akt bands. Bars are result of tree independent measurements. Error bars are standard deviations.

Figure 11. *Simplified schema of NADPH-oxidase activation.* Agonists activate G protein-coupled receptors (GPCRs) - the Gi family of heterotrimeric G proteins in hematopoietic cells. Ligand binding to receptors catalyzes liberating the Gβγ complex. Free Gβ, and Gγ subunits signals to following signal transduction pathways: (PI3Kγ)/(PIP_3)/PDK/Akt/p47phox, (Lyn,Syk)/Shc/Grb2/SOS/Ras/Raf/MEK/ERK/p47phox, PLCβ/(DAG)/PKCδ/p47phox, P-Rex/Rac, (Hck,Fgr)/Vav/Rac, PI3K/(PIP3)/DOCK-2/Rac. This leads to translocation of PHOX components to the plasma membrane and activation of NADPH-oxidase.

Table 1. Genomic effects of p66Shc knock out.

Pathways

Downregulated	Impact factor	p-value
Phosphatidylinositol signaling system	**35**	**3.2E-14**
Antigen processing and presentation	**28**	**1.4E-11**
Chronic myeloid leukemia	10	6.7E-04
Adipocytokine signaling pathway	**8**	**2.4E-03**

Upregulated	Impact factor	p-value
Glioma	10	7.6E-04
Natural killer cell mediated cytotoxicity	**9**	**8.4E-04**
ECM-receptor interaction	9	1.1E-03
Insulin signaling pathway	**6**	**1.2E-02**

Bioprocesses

Downregulated	Number of altered genes	p-value
negative regulation of programmed cell death	**6**	**3.3E-03**
anti-apoptosis	**5**	**1.2E-03**
heme biosynthetic process	**3**	**1.7E-04**
porphyrin biosynthetic process	3	3.8E-04

Upregulated	Number of altered genes	p-value
actin cytoskeleton organization and biogenesis	8	3.8E-03
actin filament-based process	8	4.4E-03
cell-matrix adhesion	4	3.1E-03
cell-substrate adhesion	4	3.7E-03

Figure 1. Peritoneal macrophages from p66Shc-/- mice have reduced PMA inducible superoxide production, trace of fluorescence increase.

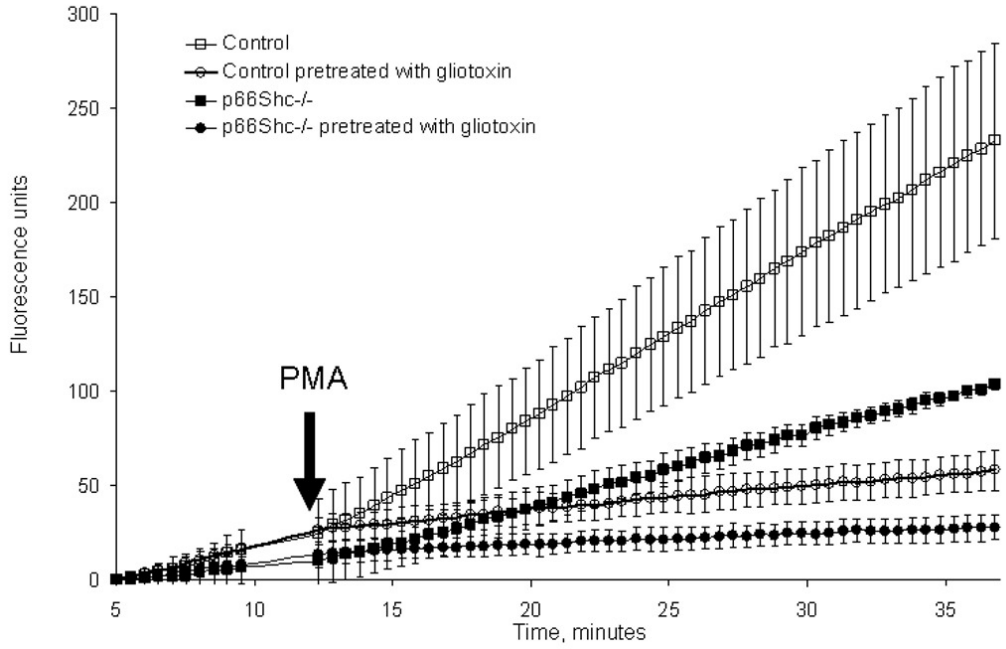

Figure 2. p66Shc-/- macrophages have defect in NAD(P)H oxidase dependent ROS generation.

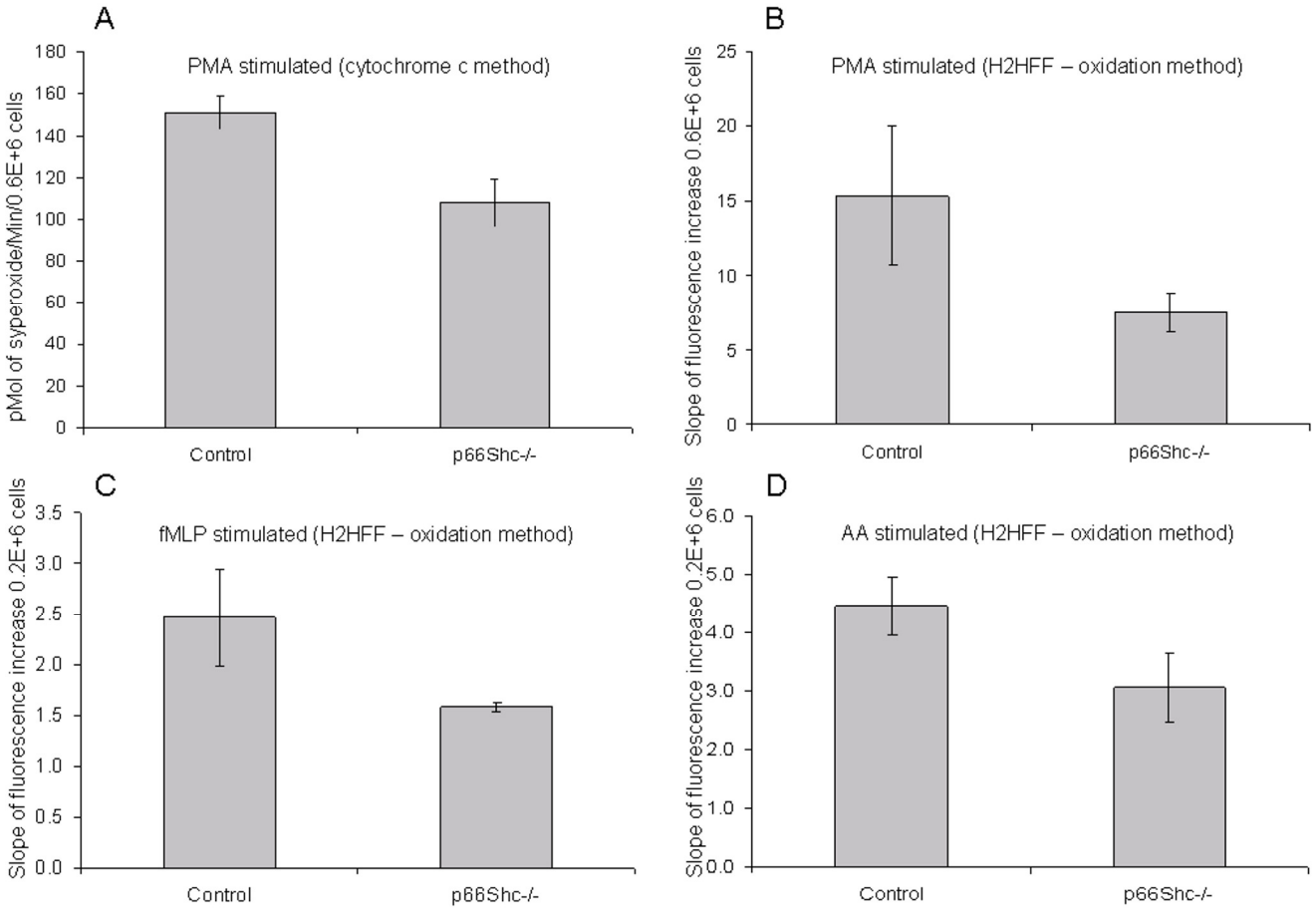

Figure 3. p66Shc-/- macrophages have no significant differences in protein levels of NOX2 subunits with respect to macrophages form control mice.

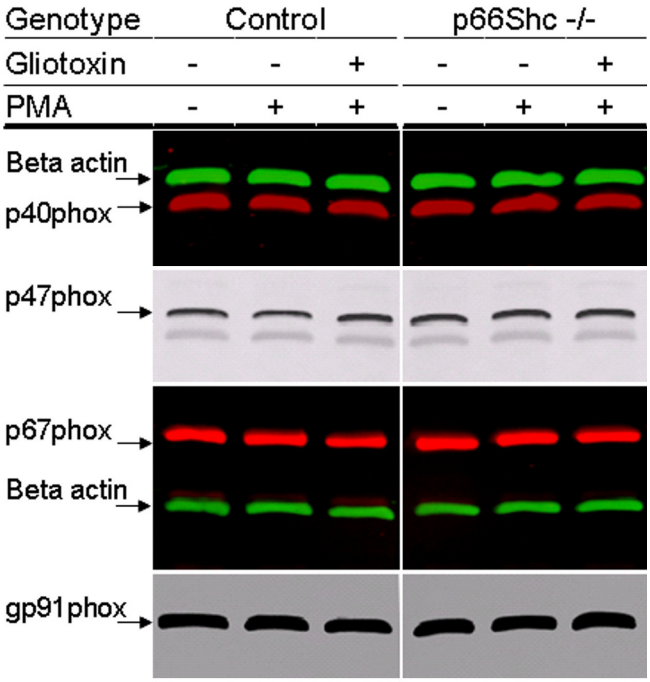

Figure 4. p66Shc -/- mice have no difference in blood heme levels from control.

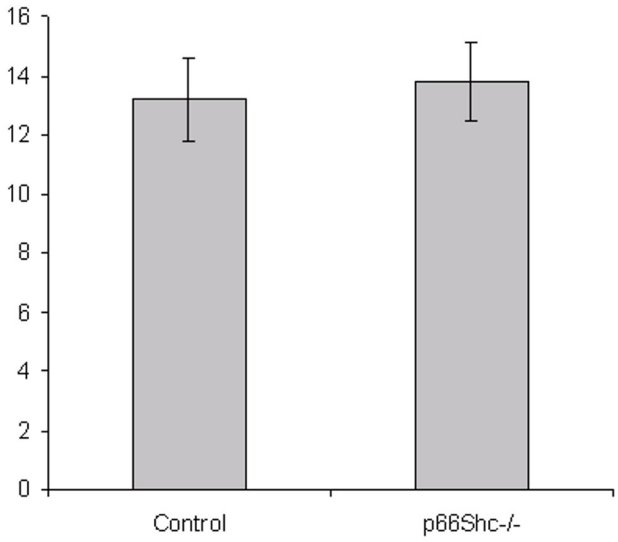

Figure 5. p66Shc-/- cells have reduced phosphorylation of p47phox.

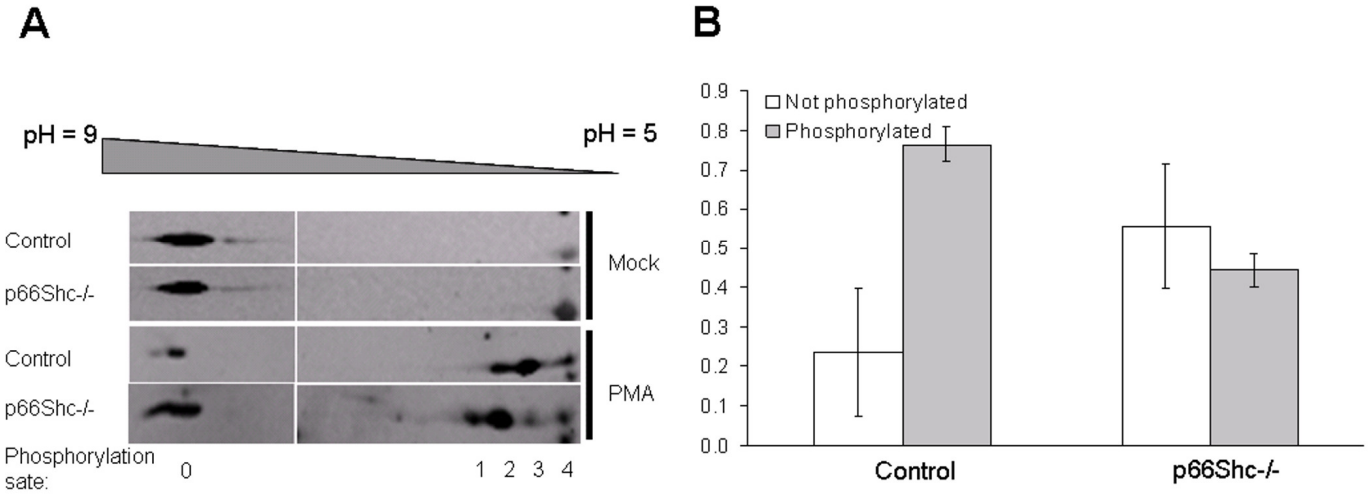

Figure 6. p66Shc-/- macrophages have defect in translocation of p47phox to membrane upon PMA induction.

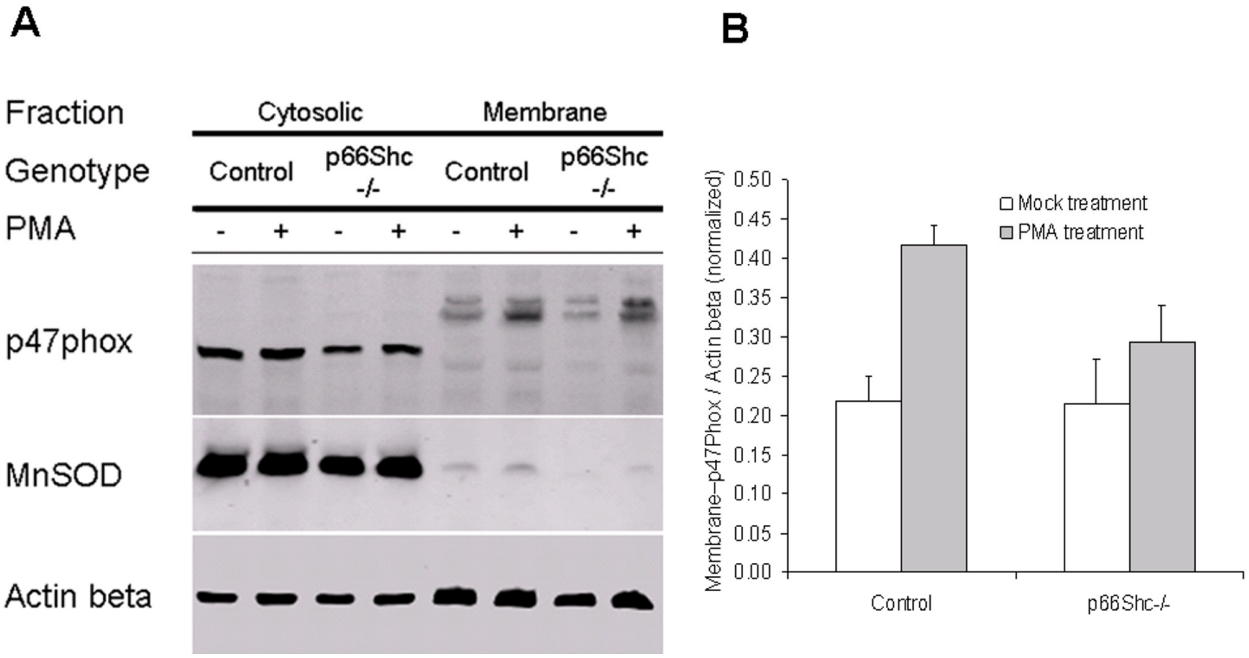

Figure 7. Mouse macrophage cell line – RAW 264.7 with siRNA – mediated p66Shc – specific knock down have defect in NAD(P)H – oxidase dependent superoxide generation.

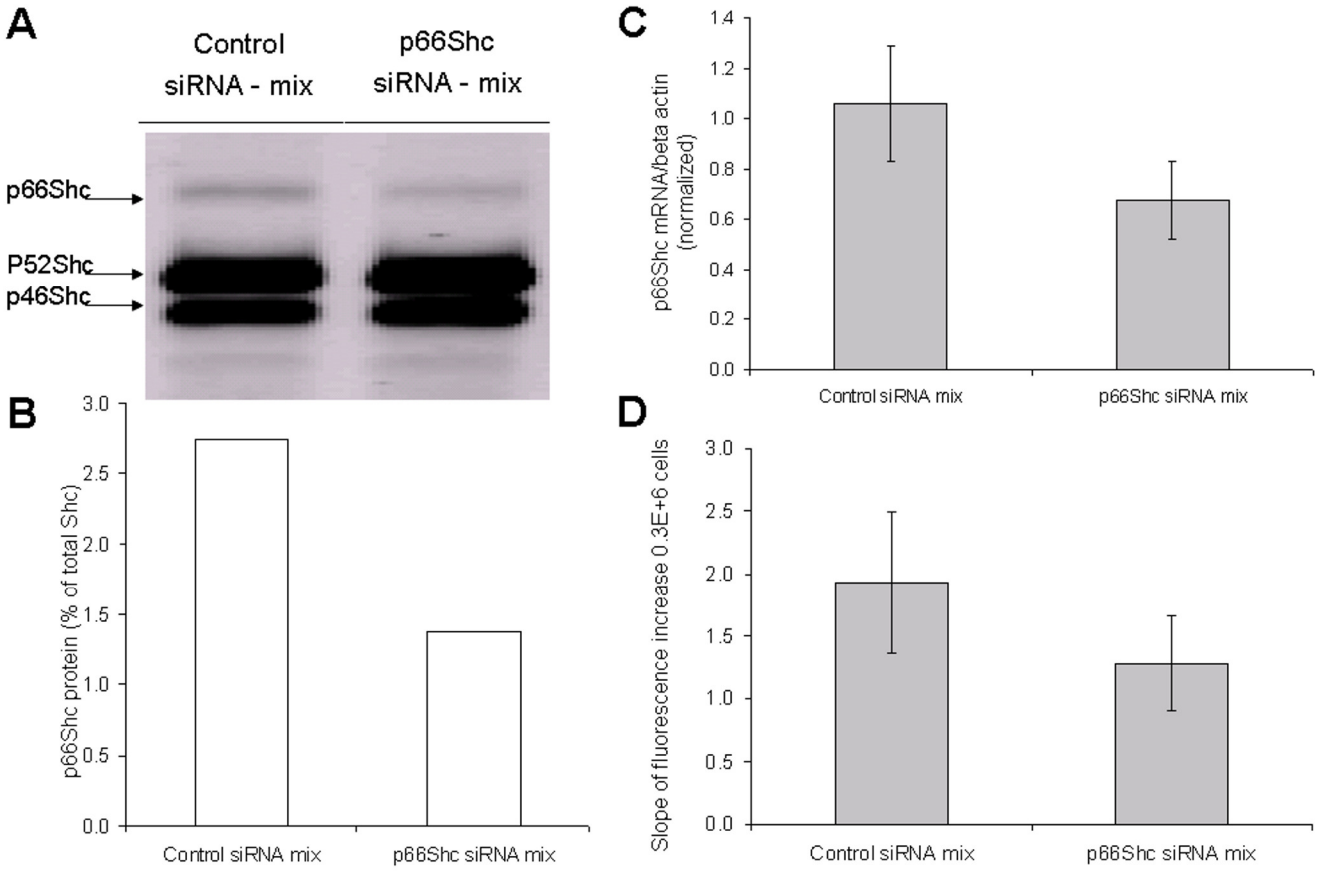

Figure 8. p66Shc(-/-) macrophages do not have a big defect in Rac1/2 activation.

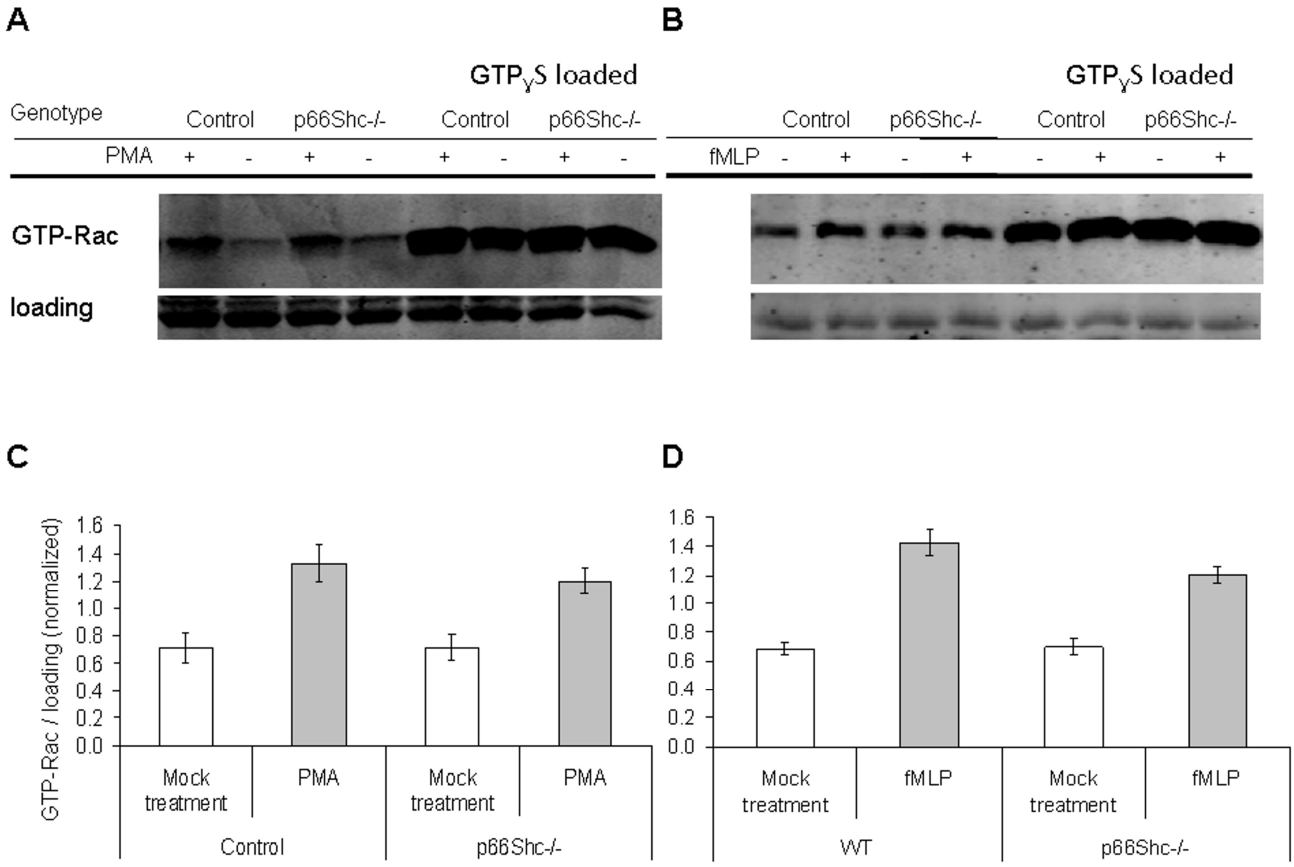

Figure 9. p66Shc-/- macrophages have reduced phosphorylation rate of PrkCδ.

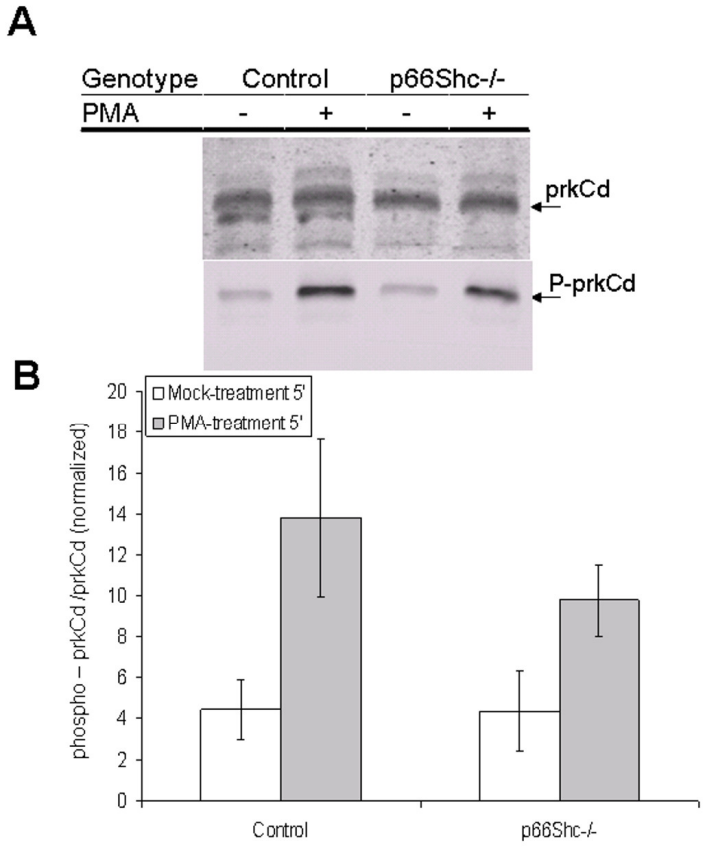

Figure 10. p66Shc-/- macrophages have reduced activation of Akt and ERK by fMLP

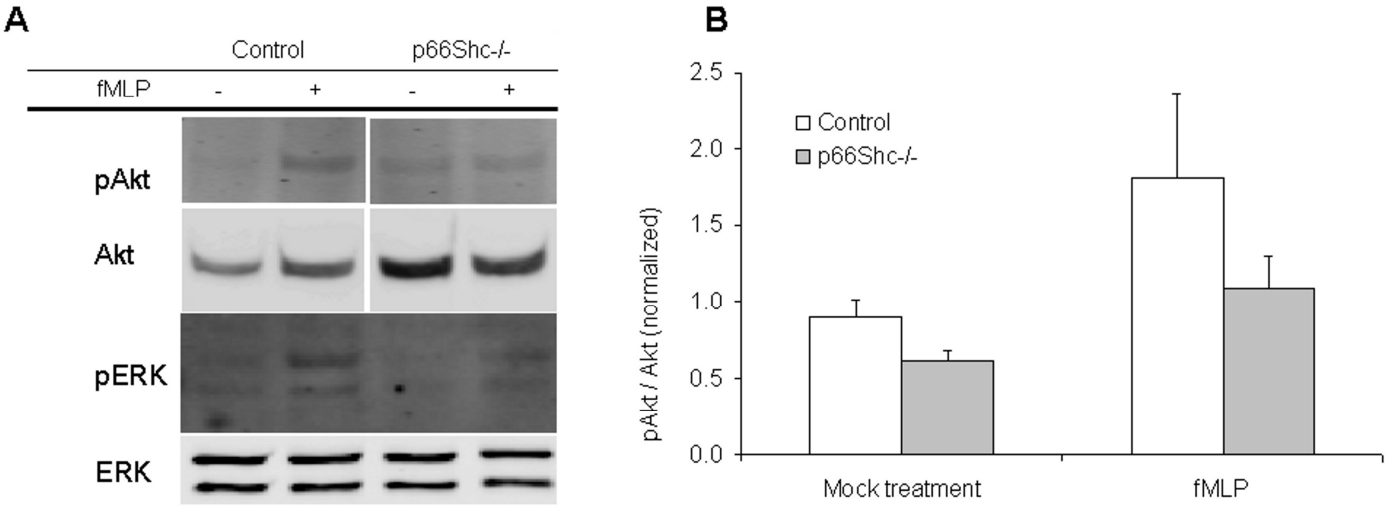

Figure 11. Simplified schema of NADPH-oxidase activation